Notes on torsion

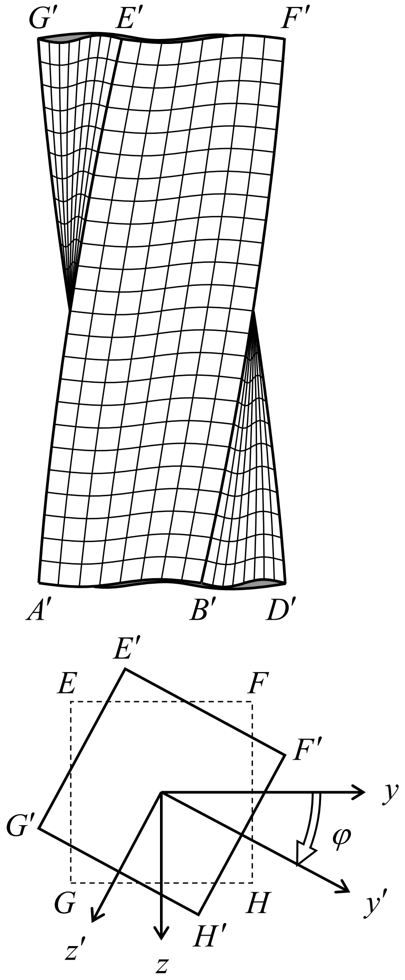

Pierre Hoogenboom

Preface

In the past, torsion was not considered in most calculations of engineering structures. Torsion was the domain of mechanical engineers who design machines with axis that transfer torsion moments. At present, we do most calculations with computers. The software tries to represent reality accurately and includes next to extension, bending and shear also torsion. We discover that torsion provides extra opportunities to fulfil the requirements of architects, contractors and subcontractors.

Important is of course that we can interpret computation results: Which part of reality is taken into account and which part is not? Is the approximation safe or do we need to correct in some situations? Important is also that we can name concepts and have discussions with others. Finally, it is important that we can check the software by calculating simple situations by hand. I hope this reader contributes to this. Perhaps also that a software developer who reads this text comes up with ideas to make our software even better.

If you have remarks, I would like to hear these. They will be processed in a following edition.

Pierre Hoogenboom
Hoogmade, 3 Augustus 2008
p.c.j.hoogenboom@tudelft.nl

2de verbeterde druk, 7 september 2010

3de verbeterde druk, 30 januari 2012

4de verbeterde druk, 26 oktober 2014

5de verbeterde druk, 18 oktober 2019

6th improved English edition, 3 January 2023

The cover figure was made by Cox Sitters [4]. The original drawing is from 1853 by Aldémar Barré de Saint-Venant [3].

Notation

A …………..	cross-section area …………………………………	mm^2
b …………...	cross-section width ………………………………..	mm
B …………..	bi-moment ………………………………………	kNm^2
C_w ………..	warping constant (Dutch: welvingsconstante) …….	mm^6
E …………...	Young's modulus (elasticiteitsmodulus) ………….	N/mm^2
EC_w ………..	warping stiffness …………………………………..	Nmm^4
G …………..	shear modulus (glijdingsmodulus) ………………..	N/mm^2
GI_t ………...	torsion stiffness ……………………………………	Nmm^2
h …………...	cross-section thickness ……………………………	mm
I_p …………	polar moment of inertia ……………………………	mm^4
I_t …………..	torsion constant or torsion moment of inertia …….	mm^4
I_{yy} ………..	bending moment of inertia in the z direction ……..	mm^4
I_{zz} ………..	bending moment of inertia in the y direction ……..	mm^4
l ……………	length of beam or column …………………………	mm
l_c …………...	characteristic length ……………………………….	mm
m_t …………	distributed torsion moment load …………………..	kNm/m
M_t …………	internal torsion moment …………………………...	kNm
p …………..	air pressure under the soap film …………………...	N/mm^2
q …………...	distributed beam load ……………………………...	kN/m
S …………..	membrane force in the soap film ………………….	N/mm
t ……………	thickness ……………………………………………..	mm
T …………...	torsion moment load ……………………………….	kNm
w …………..	altitude of a floating plate …………………………	mm
x …………..	length coordinate of the beam or column ………..	mm
y, z ……….	width coordinates of the beam or column ………..	mm
θ …………..	specific torsion …………………………………….	mm
ν …………...	Poisson's ratio (dwarscontractiecoëfficiënt) ………	-
σ …………..	normal stress ………………………………………	N/mm^2
τ …………...	shear stress ………………………………………...	N/mm^2
ϕ …………...	phi hill ……………………………………………...	N/mm
φ …………..	rotation of a cross-section …………………………	rad
ψ …………..	warping function (welvingsfunctie) ……………….	mm^2

Content

Overview

Three dimensional frame programs include torsion in the analyses. To this end the torsion stiffness of the elements must be known. When het program has computed the force flow, the stresses in the element are checked. Consequently, in this course two things are central:

1. The torsion stiffness GI_t of cross sections of prismatic structural elements such as beams and columns.

$$GI_t = ?$$

2. The distribution of torsion stresses over a cross section in particular the largest shear stress $\tau_{\max}$ in a cross-section due to the torsion moment M_t.

$$\tau_{\max} = \frac{M_t}{?}$$

Two dimensional frame programs do not include torsion because there is no torsion if there is no out of plane deformation. In two dimensional beam grids (concrete foundations) torsion can occur.

Advanced

The way in which beam ends are connected can have a large influence on the displacements and stresses due to torsion. Advanced frame programs can include this influence. For this the warping stiffness EC_w of a cross-section is important. These programs do not only draw the torsion moment line M_t but also the bi-moment line *B*. This will be addressed at the end of the course.

Learning objectives

1. Formulas for common cross sections
2. Calculation of box girders
3. Using software
4. Understanding the stress distribution and limitations of the theory
5. Becoming familiar with the scientific approach

Learning objectives 1, 2 and 3 are directly important for engineering practice. Learning objective 4 is important to evaluate computation results. Learning objective 5 is important to independently solve problems using engineering literature.

Definition

The torsion stiffness GI_t is defined by the following equation $M_t = GI_t \frac{\varphi}{l}$. In this, *l* is the length of the beam, φ is the rotation of the beam ends with respect to each other and M_t is the torsion moment (figure 1).[1]

[1] pronounce φ = fee

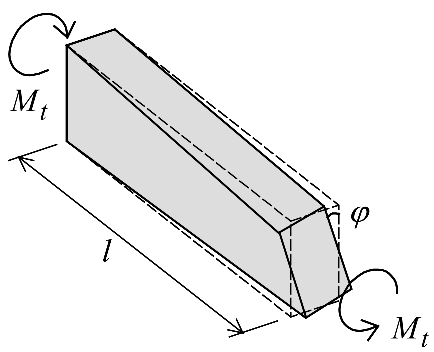

Figure 1. Deformation of a beam due to a torsion moment

Estimated torsion stiffness

For calculating the torsion stiffness GI_t, often the polar moment of inertia I_p is used. It is defined as

$$I_p = \int_A r^2 dA$$

In this, A is the cross section area and r is the distance of a point in the cross section to the centre of gravity. It can be also calculated as

$$I_p = I_{xx} + I_{yy}$$

However, the next expression is only true for circular bars and circular tubes

$$GI_t = GI_p$$

where $G = \dfrac{E}{2(1+\nu)}$ is the shear modulus. E is Young's modulus, ν is Poisson's ratio and I_t is the torsion constant.[2] For other cross sections

$$GI_t < GI_p \,.$$

Neglecting the torsion stiffness

Often, torsion contributes little to the force flow. Then the torsion stiffness can be set to zero. However, an element can contribute little to the force flow but still it must deform the same as the structure. This torsion is called compatibility torsion. The torsion moment can be considerable for this element and it is only computed correctly if a realistic torsion stiffness is used.

[2] pronounce ν = nee, many engineers say ν = nu because this is how it is written in Greek books (but not how it is pronounced by Greek people).

Reinforced concrete

Reinforced concrete beams without prestress lose much of their torsion stiffness when the concrete cracks. In figure 2 the cracked stiffness of specimen RC1-3 is only 18% of the uncracked stiffness.

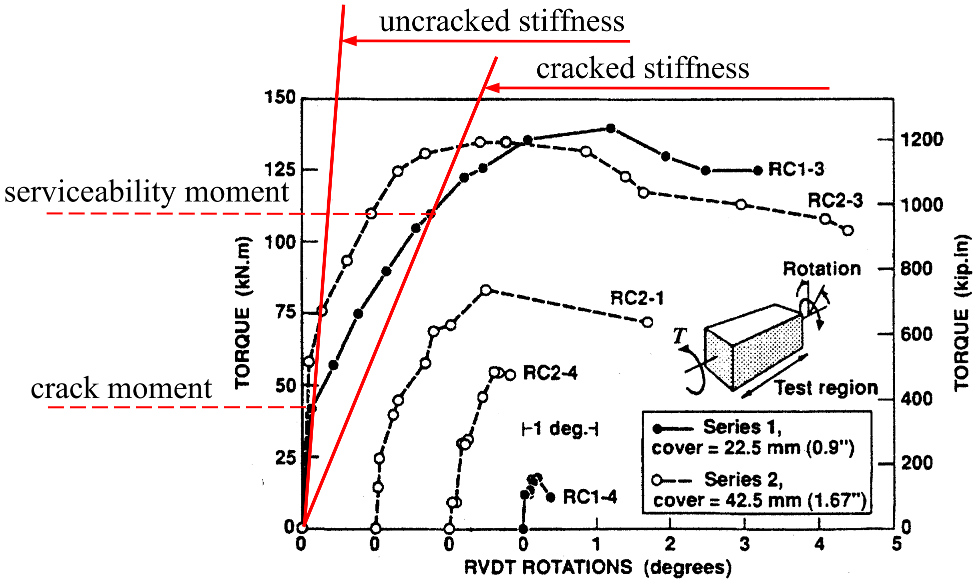

Figure 2. Experimental $M_t - \varphi$ diagrams of reinforced concrete beams [1]

For example, if a grid of foundation beams is computed with uncracked torsion stiffness, then part of the load will be carried by the torsion moment and a part by the bending moment. However, if the cracked torsion stiffness is used, small torsion moments occur and almost all load is carried by bending moments. In the latter case, we need to design more longitudinal bars but much less stirrups.

Stress distribution

Thin wall closed cross section are very suitable to carry a torsion moment because all material is used. open and solid cross sections are less suitable for torsion (figure 3). The stress distribution is often called shear flow because it looks like a small river.

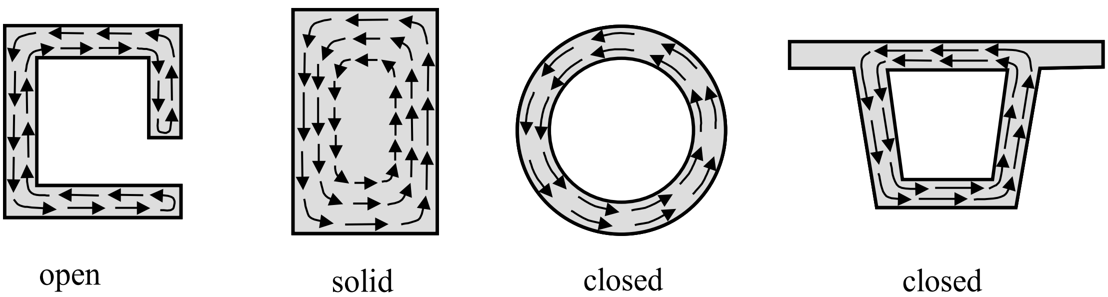

Figure 3. Torsion stresses in typical cross sections

Tables

Many design manuals have formulas for the torsion stiffness GI_t and the largest shear stress τ_{max}.[3] Particularly comprehensive is "Roark's Formulas for Stress & Strain" [2] (appendix 1). Table 1 is composed by the author using a program for cross section analysis.

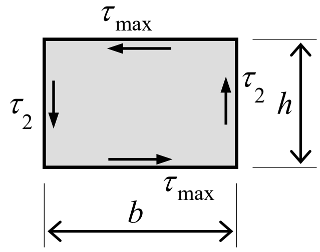

Table 1. Torsion properties of rectangular cross sections

$\frac{b}{h}$	$\frac{I_t}{bh^3}$	$\frac{I_p}{bh^3}$	$\frac{M_t}{\tau_{max} bh^2}$	$\frac{M_t}{\tau_2 bh^2}$	$1000\frac{C_w}{b^3h^3}$	$\frac{100\,B}{\sigma_{max} b^2h^2}$
1.0	0.141	0.167	0.210	0.210	0.134	0.368
1.2	0.166	0.203	0.221	0.237	0.352	0.565
1.4	0.187	0.247	0.230	0.262	0.838	0.987
1.6	0.204	0.297	0.237	0.281	1.418	1.37
1.8	0.218	0.353	0.243	0.299	2.000	1.69
2.0	0.229	0.417	0.249	0.314	2.540	1.94
2.5	0.250	0.604	0.261	0.342	3.640	2.35
3.0	0.264	0.833	0.271	0.362	4.416	2.59
4.0	0.281	1.417	0.288	0.388	5.354	2.82
5.0	0.292	2.167	0.299	0.398	5.865	2.90
10.0	0.314	8.417	0.323	0.400	6.642	2.94
50.0	0.331	208.417	0.329	0.400	6.931	2.82
∞	$\frac{1}{3}$	∞	$\frac{1}{3}$	$\frac{2}{5}$	$\frac{1000}{144}$	$\frac{100}{36}$

For example, for a cross section that is twice as wide as high $I_t = 0.229\,bh^3$ and $\tau_{max} = \dfrac{M_t}{0.249\,bh^2}$. Note that I_p is much larger than I_t. This is why I_p cannot be used to approximate I_t. (Spread the word.)

Stress check

Often the shear stress due to torsion is not the only stress in a cross section. Other stresses occur due to extension, bending and shear. The combination of these stresses should not lead to failure. For example, in steel structures we check the Von Mises stress. This is treated in other courses.

Warping

Warping is the deformation of an initially plane cross section. In Dutch it is called "welving". It occurs due to a torsion moment and also due to a shear force.

[3] pronounce τ = taf with an "a" as in car. Many engineers say τ = tau

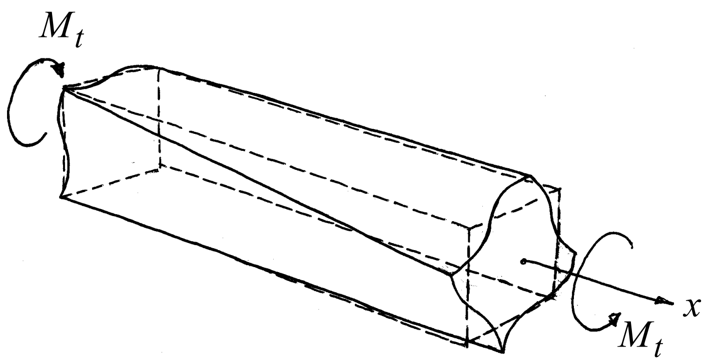

Figure 4. Warping of square beam ends due to torsion

Theory of Saint-Venant

In 1856, Aldémar Barré de Saint-Venant [4] published a theory for torsion [3]. It starts from the assumption that a cross section rotates around the x axis and warps in the x direction (figure 5, rotation is shown, warping is not)

$$u_y = -zx\theta$$
$$u_z = \quad yx\theta$$
$$u_x = \psi(y,z)\theta$$

In this, $\theta = \dfrac{\varphi}{l}$ is the specific torsion and ψ is the warping function, which describes the warping of the cross section.[5] The assumption is only realistic for small θ.

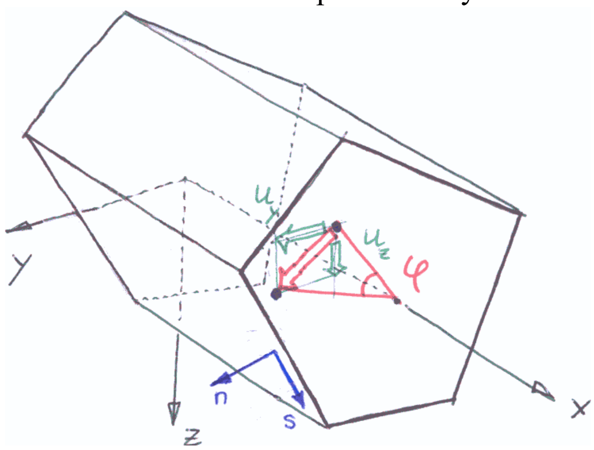

Figure 5. Displacement of an arbitrary point due to a small rotation φ of a cross section (warping is not shown)

Exercise: Check whether Sant-Venant's assumption makes sense.

Displacement method

In the displacement method we select the warping as an unknown function. The result of the derivation [4] is the partial differential equation

[4] A.J.C. Barré de Saint-Venant (1797 – 1886) was a French civil engineer. Later in live he was a mathematics professor at the École des Ponts et Chaussées [Wikipedia].
[5] pronounce θ = teta , φ = fee, ψ = psee

$$\frac{\partial^2\psi}{\partial y^2}+\frac{\partial^2\psi}{\partial z^2}=0$$

with boundary condition

$$\frac{\partial\psi}{\partial n}=z\cos\alpha-y\sin\alpha$$

where α is the angle between the positive y axis and the outward normal vector on the edge in the considered point.[6] If ψ is solved, the stresses can be calculated with

$$\tau_{xy}=G\left(\frac{\partial\psi}{\partial y}-z\right)\theta$$
$$\tau_{xz}=G\left(\frac{\partial\psi}{\partial z}+y\right)\theta$$

and the torsion moment with

$$M_t=\int_A(y\,\tau_{xz}-z\,\tau_{xy})dA\,.$$

The torsion stiffness is

$$GI_t=\frac{M_t}{\theta}\,.$$

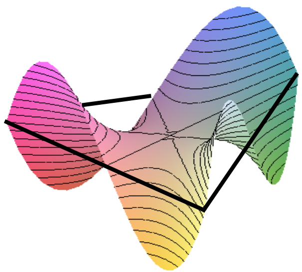

Figure 6. Warping function $\psi(y,z)$ of a triangular cross section.
Mathematicians call this function a monkey saddle.

Force method

In the force method we choose the stresses as unknown functions. The result of the derivation [4] is the partial differential equation

$$\frac{\partial^2\phi}{\partial y^2}+\frac{\partial^2\phi}{\partial z^2}=-G2\theta$$

and the boundary conditions

[6] pronounce α = alfa

$$\frac{\partial \phi}{\partial s} = 0 .$$

The function $\phi(y,z)$ has no direct physical meaning.[7] The function has the shape of a hill and therefore it is called ϕ–hill (figure 7).[8] If ϕ is solved we can calculate the torsion stresses with

$$\tau_{xy} = \frac{\partial \phi}{\partial z}$$
$$\tau_{xz} = -\frac{\partial \phi}{\partial y} .$$

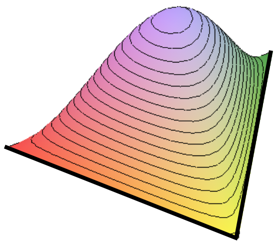

Figure 7. ϕ–hill of a triangular cross section

The shear stress in random perpendicular directions *n* and *s* can be calculated in the same way

$$\tau_{xn} = \frac{\partial \phi}{\partial s}$$
$$\tau_{xs} = -\frac{\partial \phi}{\partial n}$$

and the torsion moment with

$$M_t = 2\int_A \phi \, dA .$$

The torsion stiffness is

$$GI_t = \frac{M_t}{\theta} .$$

Internal edge

A cross section of a box girder does not only have an external edge but also one or more internal edges. It can be proven that for each of the internal edges holds [4, p. 186]

[7] pronounce ϕ = fee (Greek capital letter)
[8] pronounce fee-hill

$$\int_s \sigma_{xs} ds = -2GA_g\theta$$

where s is the considered internal edge and A_g the accompanying opening area of the cross section. This result is required in the calculation of multi-cell box girder bridges.

Exact solutions

The differential equations can be solved analytically for four cross sections (table 2). More exact solutions have not been found. Note that circular sections do no warp.

Table 2. Four exact solutions of the differential equations

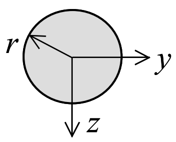	$\psi = 0$ $\phi = \frac{1}{2}G\theta(r^2 - y^2 - z^2)$	$I_t = I_p = \frac{1}{2}\pi r^4$ $C_w = 0$ $\tau_{max} = \frac{M_t}{\frac{1}{2}Ar}$ $\sigma_{max} = 0$
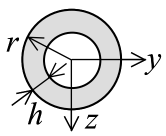	$\psi = 0$ $\phi = \frac{1}{2}G\theta(r^2 - y^2 - z^2)$	$I_t = I_p = \frac{1}{2}\pi(r^4 - (r-h)^4)$ $C_w = 0$ $\tau_{max} = \frac{r\, M_t}{I_t}$ $\sigma_{max} = 0$
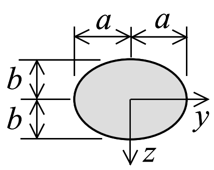	$\psi = zy\frac{b^2 - a^2}{b^2 + a^2}$ $\phi = G\theta\frac{a^2b^2}{a^2+b^2}(1 - \frac{y^2}{a^2} - \frac{z^2}{b^2})$	$I_t = \frac{\pi a^3 b^3}{a^2 + b^2}$ $I_p = \frac{1}{4}\pi ab(a^2 + b^2)$ $C_w = \frac{\pi a^3 b^3}{24}\frac{(a^2-b^2)^2}{(a^2+b^2)^2}$ $\tau_{max} = \frac{M_t}{\frac{1}{2}\pi ab^2}$ $\sigma_{max} = \frac{\pi a^2 b^2}{12}\frac{a^2 - b^2}{a^2 + b^2}B$
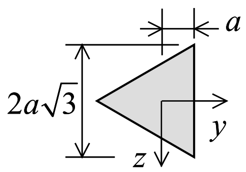	$\psi = \frac{z}{6a}(3y^2 - z^2)$ $\phi = \frac{G\theta}{6a}(a-y)(2a+y-z\sqrt{3})(2a+y+z\sqrt{3})$	$I_t = \frac{9}{5}\sqrt{3}\,a^4$ $I_p = 3\sqrt{3}\,a^4$ $C_w = \frac{3}{70}\sqrt{3}\,a^6$ $\tau_{max} = \frac{M_t}{\frac{6}{5}\sqrt{3}a^3}$ $\sigma_{max} = \frac{B}{\frac{9}{70}\sqrt{3}a^4}$

Finite element method

The finite element method can be used to solve the differential equations with ψ or ϕ for every cross section shape[9]. To this end the cross section is divided in a large number of quadrilateral and triangular elements. There are many programs that can perform the computation. Examples are

ShapeDesigner	http://mechatools.com
ShapeBuilder 3.0	http://www.iesweb.com

The program user can set the size of the elements. This can be used to check the accuracy of the computation: Repeat the computation with elements of about halve size. If the computation results do not change much, it is sufficiently accurate. If the results do change much, the elements are too large. We do not need to be economical with the number of elements because even a mesh with 10 000 elements is computed in seconds on a modern PC.

Most frame programs have libraries of standard sections, in which torsion constants I_t are included. Therefore, these do not need to be computed. However, if we design a cross section, than I_t must be computed. SCIA Engineer has a module that automatically computes the torsion constant I_t of any cross section with the finite element method. The structural engineer needs to choose for this computation. If he or she does not, the program does the structural analysis with the polar moment of inertia I_p. This would give completely wrong results (Compare I_t with I_p in table 1).

Example of a rectangular cross section

We consider a timber beam with a rectangular cross section.

depth = 400 mm	
width = 200 mm	
Young's modulus	E = 10000 MPa
Poisson's ratio	$\nu = 0.1$
torsion moment	$M_t = 100\,\text{kNm}$
shear modulus	$G = \dfrac{E}{2(1+\nu)} = \dfrac{10000}{2(1+0{,}1)} = 4545\ \text{MPa}$

We use **table 1**. In this table *h* is always smaller than *b*. So *h* = 200 and *b* = 400.

[9] The development of the finite element method got off the ground in 1960. In this year the civil engineers Ray Clough (1920 – 2016) and Edward Wilson (1931 –) wrote a computer program that computed the stresses in dams. They worked in the University of California at Berkeley. The program was applied to the Norfork dam, which controls a lake in Arkansas, USA. In the middle of this dam a large vertical crack had occurred. The finite element computation showed that the dam was safe despite the crack. The dam did not need to be replaced [21]. The success got the attention of mathematicians. They developed the method further to solve arbitrary differential equations.

One can say that the mathematician stole our finite element method, remodeled it unrecognisably and gave it back, so that we can solve the differential equations of Saint-Venant.

$$GI_t = 0.229bh^3G = 0,229 \times 400 \times 200^3 \times 4545 = 333 \times 10^{10}\,\text{Nmm}^2$$

$$\tau_{\max} = \frac{M_t}{0.249bh^2} = \frac{100 \times 10^6}{0.249 \times 400 \times 200^2} = 25.1\,\text{MPa}$$

Exercise: What happens if you accidentally exchange h and b ?

We can determine GI_t and $\tau_{\max}$ in another way. According to **Roark's formulas** (appendix 1)

a = 400/2 = 200
b = 200/2 =100

$$GI_t = Gab^3\left[\tfrac{16}{3} - 3.36\frac{b}{a}\left(1 - \frac{b^4}{12a^4}\right)\right]$$

$$= 4545 \times 200 \times 100^3\left[\tfrac{16}{3} - 3.36\frac{100}{200}\left(1 - \frac{100^4}{12 \times 200^4}\right)\right] = 333 \times 10^{10}\,\text{Nmm}^2$$

$$\tau_{\max} = \frac{3M_w}{8ab^2}\left[1 + 0.6095\frac{b}{a} + 0.8865\frac{b^2}{a^2} - 1.8023\frac{b^3}{a^3} + 0.9100\frac{b^4}{a^4}\right]$$

$$= \frac{3 \times 100 \times 10^6}{8 \times 200 \times 100^2}\left[1 + 0.6095\frac{100}{200} + 0.8865\frac{100^2}{200^2} - 1.8023\frac{100^3}{200^3} + 0.9100\frac{100^4}{200^4}\right]$$

$$= 25.46\ \text{MPa}$$

The third and last way to determine GI_t and $\tau_{\max}$ is by the finite element method. The program **SCIA Engineer** produces (See figures 8, 9, 10 and 11):

$$I_t = 730175100\ \text{mm}^4$$

$$GI_t = 4545 \times 730175100 = 331.9 \times 10^{10}$$

$$\tau_{\max} = 2.55 \times 10^{-4}\ \text{MPa}$$

The torsion stiffnesses that are determined with the three methods agree well.
The largest stress determined by table 1 and Roark's formulas agree well too. The largest stress computed by SCIA Engineer is much too small. Apparently, this stress needs to be multiplied with $10^{-3}M_t$. This is caused by the philosophy of the program. After all, in this phase of a structural analysis, the moments are not known.

Note: In figure 9, the altitude lines have negative values. So, we are looking at a ϕ – valley instead of a ϕ –hill. For the principle this does not matter.

Note: The figures also show buttons that are related to shear stiffness and the stresses due to a shear force. For this is also a differential equation. This subject is not covered in these notes.

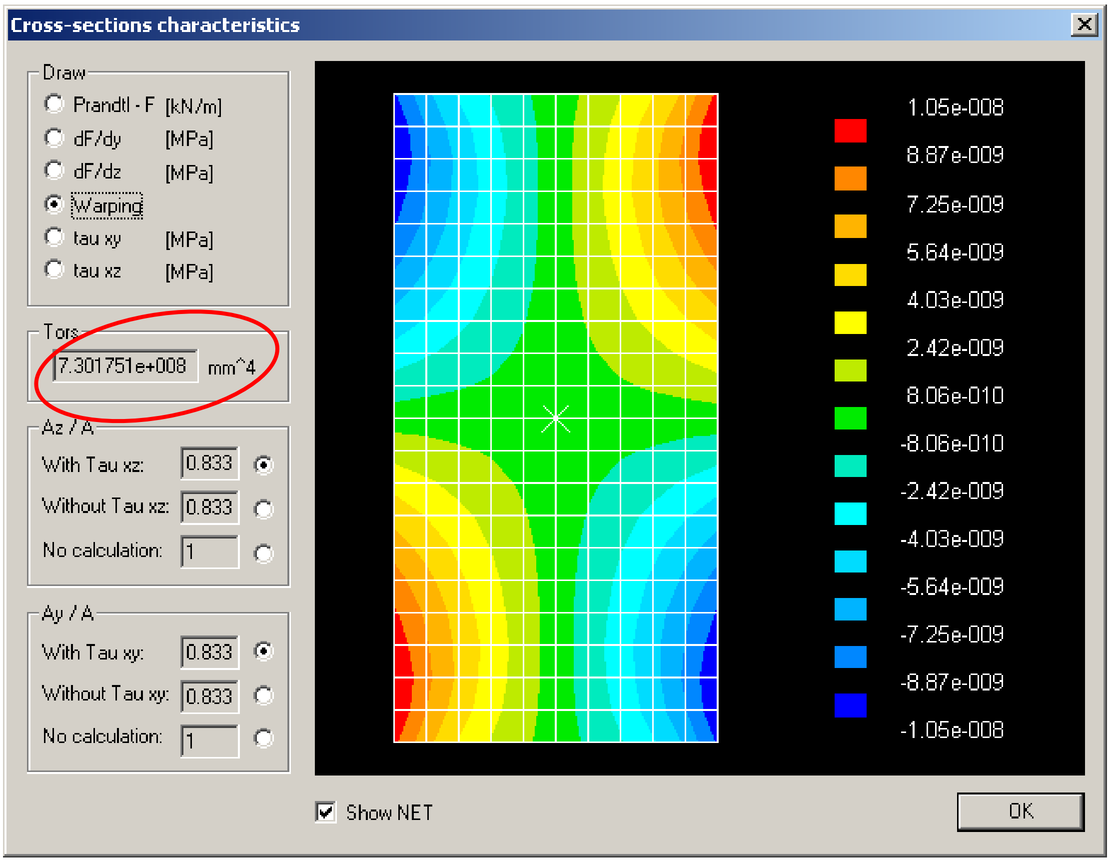

Figure 8. Element mesh and warping of the cross section

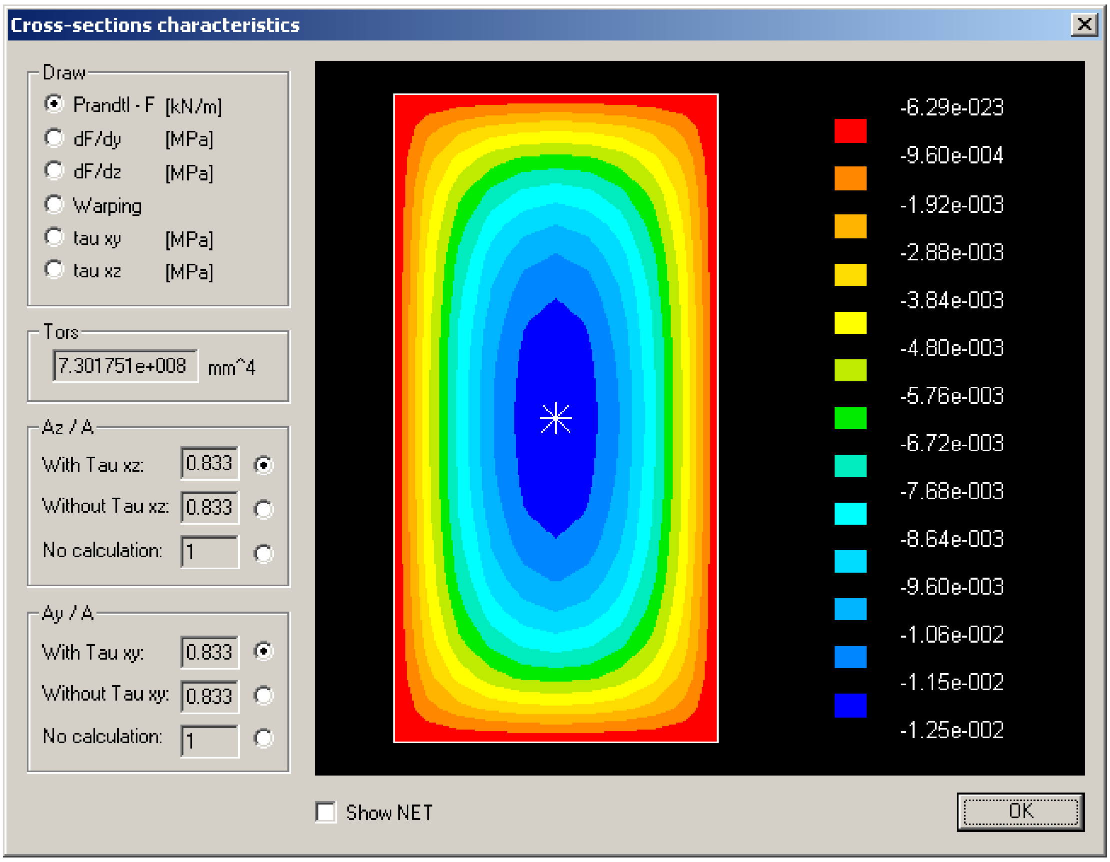

Figure 9. ϕ–hill

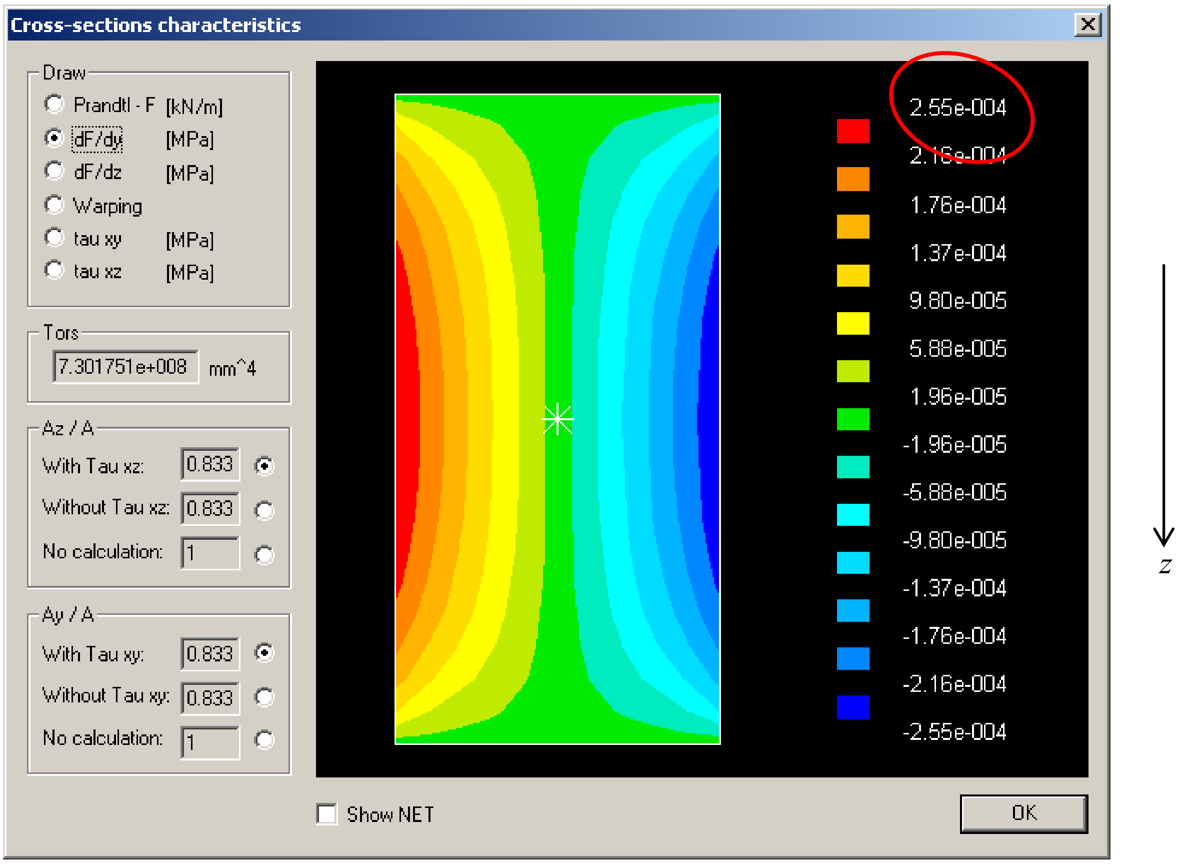

Figure 10. Shear stresses τ_{xz} in the z direction of the cross section

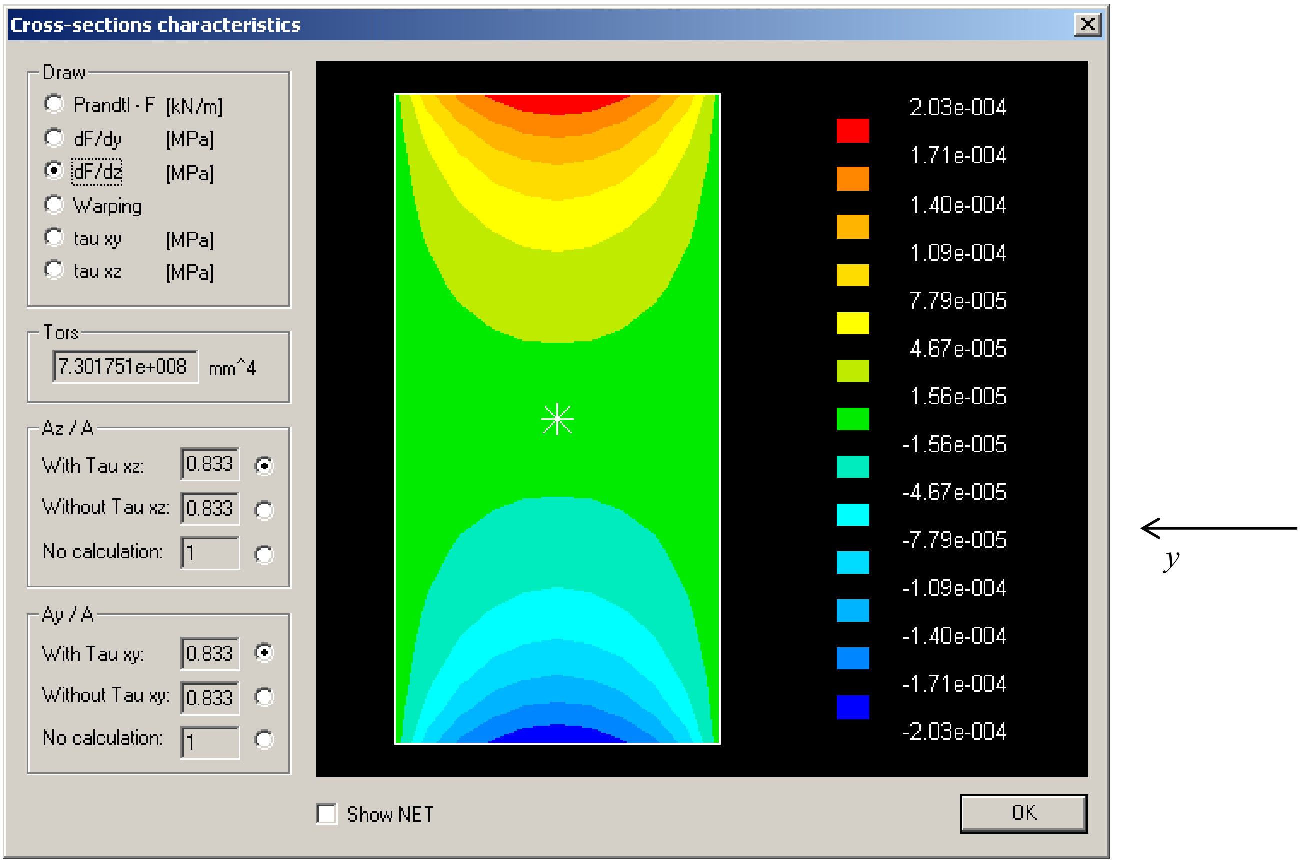

Figure 11. Shear stresses τ_{xy} in the y direction of the cross section

Interpretation of the ϕ–hill

A top view of the ϕ –hill gives much qualitative information on de distribution of the shear stresses. In a certain point the direction of the shear stress is equal to the direction of the altitude line (figure 12). The magnitude of the shear stress is inversely proportional to the distance between the altitude lines. Therefore, the altitude lines are stress trajectories. Large stresses occur where the altitude lines are close to each other.

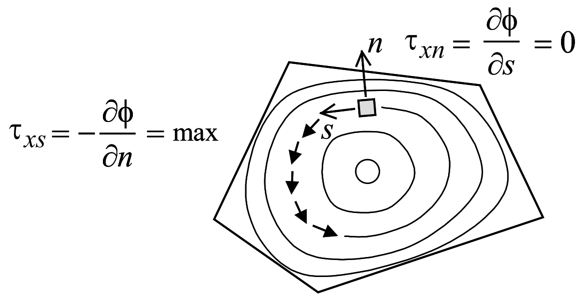

Figure 12. Relation between the stresses and the altitude lines of the ϕ –hill

Estimated torsion stiffness

A formula exists for estimating the torsion stiffness of squat cross sections [5].

$$GI_t \approx \frac{GA^4}{4\pi^2 I_p}$$

In this A is the cross section area. The word squat means here that the cross section is not elongated, has no thin parts and has no parts sticking out. Examples are, square cross sections (8% to large), solid round cross sections (exact) and cross sections shaped as an equilateral triangle (14% to large). The formula can be derived by rewriting the solution for an ellipse cross-section (table 2).

Thin wall open cross sections

Formulas exist for thin strips and thin wall open cross sections.

Strip

$$GI_t = G\tfrac{1}{3}bh^3$$

$$\tau_{\max} = \frac{M_w}{\tfrac{1}{3}bh^2}$$

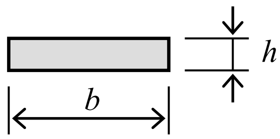

Thin wall open cross section

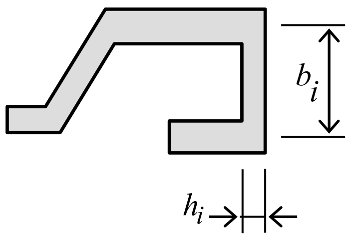

$$GI_t = \sum_i G_i \tfrac{1}{3} b_i h_i^3$$

$$\tau_j = \frac{GI_{tj}}{GI_t} \frac{M_t}{\tfrac{1}{3} b_j h_j^2}$$

More accuracy can be obtained by replacing $\frac{1}{3}$ by numbers from table 1.
If G is the same for all parts, the latter formula simplifies into

$$\tau_j = \frac{M_t\, h_j}{I_t}$$

Exercise: Derive this formula.

Example of a balustrade

A glass balustrade has a wooden hand rail (see figure 13). The connection is glued.
The shear modulus of glass is

$$G = \frac{E}{2(1+\nu)} = \frac{70000}{2(1+0.2)} = 29167 \text{ N/mm}^2$$

The torsion stiffness of the glass is

$$GI_t = 29167\, \tfrac{1}{3} 1320 \times 20^3 = 103 \cdot 10^9 \text{ Nmm}^2$$

The torsion stiffness of the wood is

$$GI_t = 4000 \times 0.207 \times 100 \times 60^3 = 17.9 \cdot 10^9 \text{ Nmm}^2$$

In total $GI_t = 121 \cdot 10^9$ Nmm².

The balustrade is loaded by a torsion moment of 2 kNm. The largest shear stress in the glass is

$$\tau = \frac{103}{121} \frac{2 \cdot 10^6}{\frac{1}{3} 1320 \times 20^2} = 9.7 \text{ N/mm}^2$$

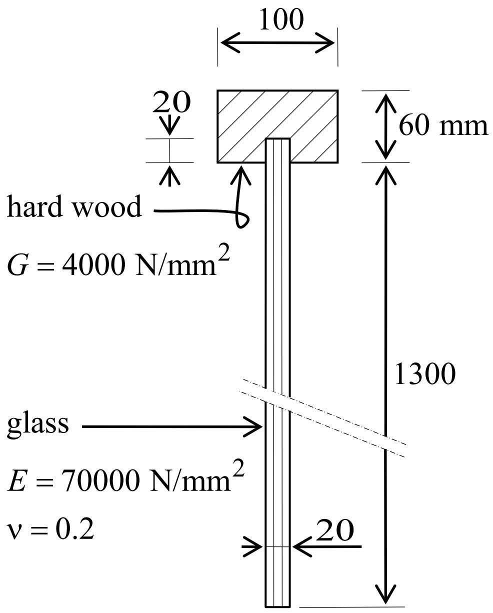

Figure 13. Balustrade with hand rail

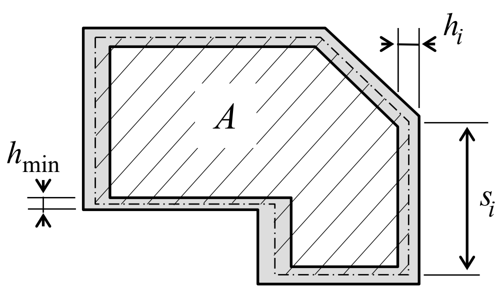

Figure 14. Box girder

The largest shear stress in the wood cannot be calculated by hand because this is influenced by the connection with the glass. In the top of the hand rail the shear stress is approximately

$$\tau = \frac{17.9}{121} \frac{2 \cdot 10^6}{0.239 \times 100 \times 60^2} = 3.4 \text{ N/mm}^2$$

Formulas by Bredt

In 1896, Rudolph Bredt derived two convenient formulas for closed thin wall beams that have just one cell [6] (figure 14). [10]

$$GI_t = \frac{4A^2}{\sum_i \frac{s_i}{G_i h_i}} \qquad \text{(Bredt's second formula)}$$

$$\tau_j = \frac{M_t}{2Ah_j} \qquad \text{(Bredt's first formula)}$$

Exercise: In closed cross sections the largest shear stress occurs in the thinnest wall, while in open cross sections the largest shear stress occurs in the thickest wall. What causes this?

Membrane analogy

The differential equation of the force method is the same as that of a soap film. This was first used by Ludwig Prandtl in 1903 [7].[11] The differential equation of a soap film is

$$\frac{\partial^2 w}{\partial y^2} + \frac{\partial^2 w}{\partial z^2} = -\frac{p}{S} .$$

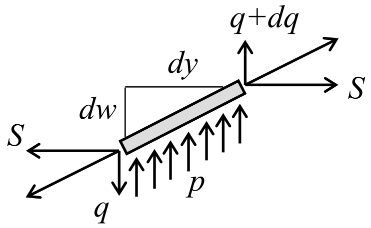

In this, S is the horizontal tensile force in the film and p is the over pressure under the film. The boundary condition is $w = 0$ on the edge.

Thus we can interpret the ϕ–hill as a soap film over an open box. The top view of the box has the shape of the cross section of the beam. There is overpressure in the box, which makes the film bulge.

Often this is called "membrane analogy". This name is an unfortunate choice because a membrane can have different stresses in different directions. A soap film has in all directions the same stress.

[10] Rudolph Bredt (1842 – 1900) was a structural designer. He was in charge of the first crane building company of Germany in Wetter an der Ruhr (DEMAG)[22].

[11] Ludwig Prandtl (1875 – 1953) was a professor in Göttingen, Germany. He also did groundbreaking research in flow around ships and airplanes and he was active in both world wars [Wikipedia].

When comparing the soap film differential equation (p. 15) to the ϕ –hill differential equation (p. 6), we notice that the tensile force S in the soap film can be related to the shear modulus G of the beam material. The overpressure p in the box can be related to the specific torsion θ of the beam.

$$w = \phi$$
$$S = \frac{1}{G}$$
$$p = 2\theta$$

Membrane analogy for box girders

The cross section of a closed box beam has not only an external edge but also one or more internal edges. On each of the internal edges, there are two conditions for the soap film

$$\frac{\partial w}{\partial s} = 0$$
$$S\int_s \frac{\partial w}{\partial n} ds = pA_g\,.$$

In this, s is the considered internal edge and A_g is the considered area of the cross section opening. The last formula can be derived from the formula on the top of page 8. This means that the value of w is constant on an internal edge. Moreover, the vertical resultant of the soap film force over the internal edge is equal to the overpressure p times the area A_g of the opening.

Figure 15 shows the interpretation: A horizontal weightless plate shaped as the opening, hovers above the opening. The soap film is attached to the plate edge. The soap film pulls the plate down the overpressure pushes the plate up.

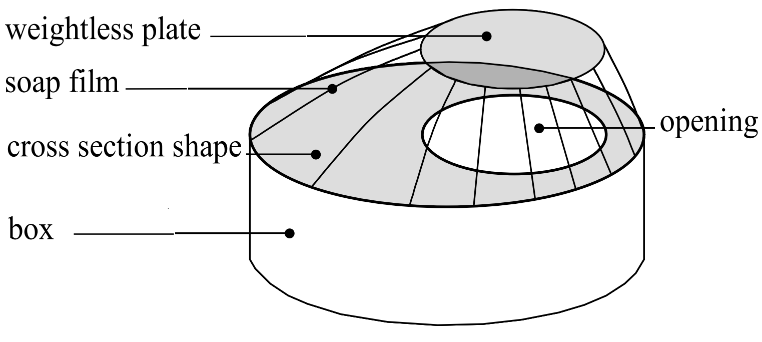

Figure 15. Weightless plate as internal boundary condition

Application of the membrane analogy

The membrane analogy is very suitable for manual calculation of the ϕ –hill of box girders (thin wall, closed, multiple cells). The altitudes of the weightless plates are calculated from equilibrium. The girder walls are thin, therefore, the curvature of the soap film is neglected. The force q [N/m] that pulls down the weightless plate edges follows from the slope of the film. It is customary to take all dimensions to the centre lines of the walls. This strongly reduces the amount of calculation work and prevents calculation mistakes. The calculation is demonstrated in appendix 2.

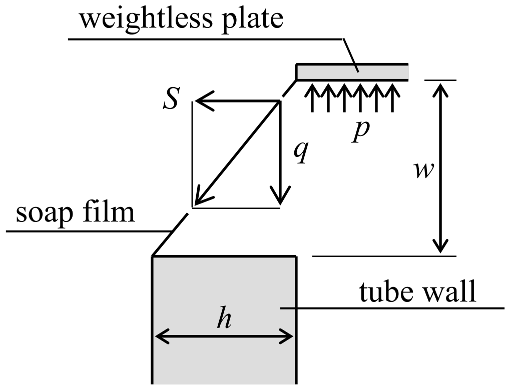

$$\frac{q}{S} = \frac{w}{h}$$

Figure 16. Forces on a weightless plate

Nabla girder [12]

The membrane analogy can be used to analyse a nabla girder (appendix 3). The result is

$$GI_t = G\,\frac{9}{4}\,a^3 h$$

$$\tau_{\max} = \frac{4}{27}\sqrt{3}\,\frac{M_t}{a^2 h}$$

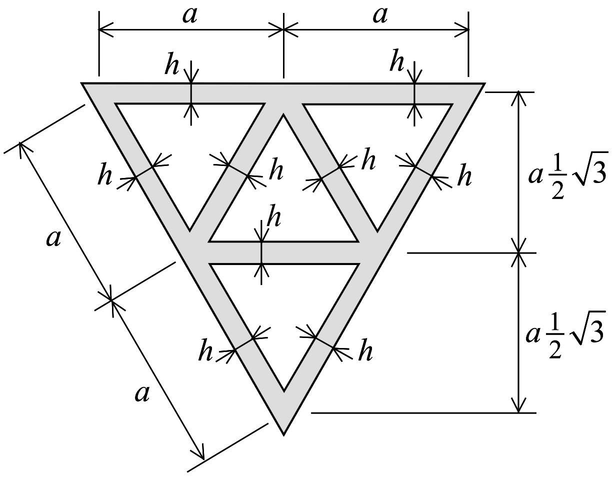

Hollow core slab

The membrane analogy can be used to analyse a hollow core slab (appendix 4). The round channels are modelled square to make the hand calculation possible. The middle webs are left out of the model because these contribute little.

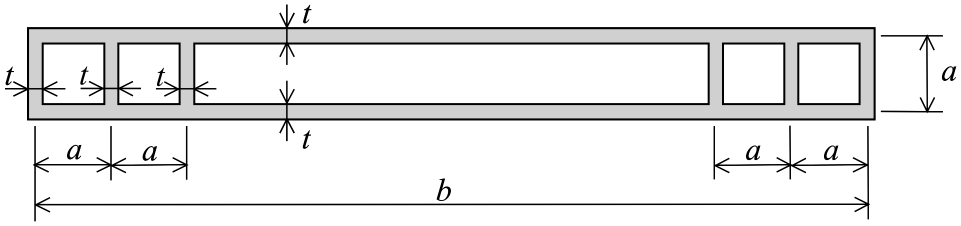

$b \geq 5a$

[12] The symbol ∇ is pronounced nabla. It is often used in mathematics.

$$GI_t = 6\frac{5b^2 - 20ab + 12a^2}{15b - 49a}Ga^2t$$

$$\tau_{\max} = \frac{1}{6}\frac{15b - 50a}{5b^2 - 20ab + 12a^2}\frac{M_t}{at}$$

The largest shear stress in the cross section occurs in the middles of the top and bottom edges.

This hollow core slab model is clearly a rough approximation of reality. The real torsion stiffness is larger (the author estimates 60% larger). The real largest shear stress can be larger or smaller (the author estimates 30% larger). For accurate values we need to do a finite element analysis.

Sand hill analogy

There is also an analogy for plastic analysis of torsion properties. The plastic ϕ–hill looks like a sand hill. For an experiment, we cut a plate in the shape of the cross section. Subsequently, we sprinkle dray sand on the plate until the shape of the hill does not change any longer (figure 17).

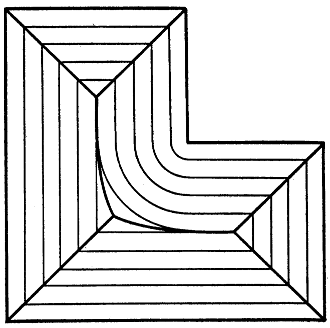

Figure 17. Plastic ϕ–hill of an L shaped cross section, top view [8]

Stress concentrations

Stress concentrations occur in re-entrant corners of cross sections. After all, here the ϕ–hill has a larger slope. Often it is necessary to round re-entrant corners. A formula by Trefftz approximates the stress in a 90°-corner of a box girder (figure 18) [9]. [13]

$$\tau_{\max} = 1.74\sqrt[3]{\frac{h}{r}}\,\tau$$

In this, r is the radius of the rounding, h is the wall thickness and τ is the shear stress at some distance of the corner. This formula is not accurate but on the safe side [10]. The stress concentration is important in fatigue calculations.

[13] Erich Trefftz (1888 – 1937) was a structural mechanics professor in Dresden. He was a good friend of Richard von Mises who had to leave Germany in 1933 because he was Jewish [German Wikipedia].

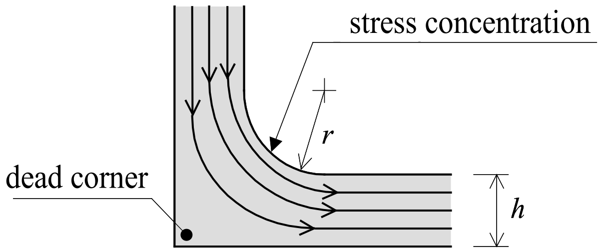

Figure 18. Stress concentration in a 90° corner

Shear centre

The shear centre is a point in the cross section of a beam. If a force goes through the shear centre, it will not produce a torsion moment. The shear centre coincides with the centre of gravity in cross sections that are double symmetrical, for example in a rectangular cross section or in an I section (appendix 5). In other cross sections it does not coincide, for example a U section (figure 19 and 20).

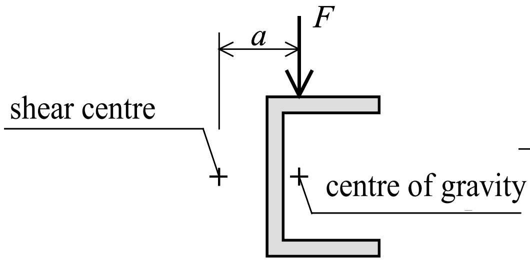

Figure 19. Torsion moment Fa

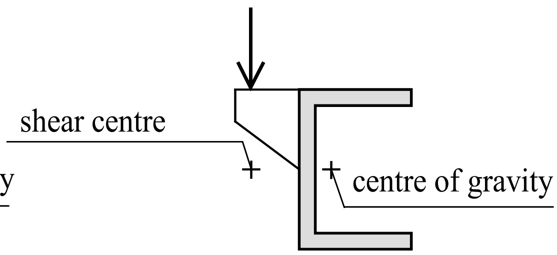

Figure 20. No torsion moment

The place of the shear centre is calculated from the distribution of shear stresses in a cross section due to a shear force. This calculation is not treated in this course.

Rotation

Above is not mentioned around which point the cross sections rotate. From figure 5 we can get the impression that the x axis goes through the centre of gravity. However, it can be proven that the position of the x axis does not have an influence on the calculated torsion stiffness or the calculated torsion stresses. The theory of Saint-Venant does not tell us around which point a cross section rotates.

Theorem
A torsion moment rotates the cross sections around the shear centre.

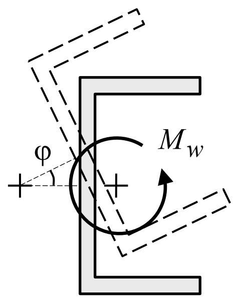

Proof
This can be simply proven for linear elastic beams. A force through the shear centre gives a rotation $\varphi = 0$ of each point of a cross section. From reciprocity (symmetry of the stiffness matrix) follows that a torsion moment on an arbitrary point of the cross section gives a displacement $u = 0$ of the shear centre. So, the cross section rotates around the shear centre.

Orthotropic plate

A bridge or floor that consists of parallel beams is often modelled as an orthotropic plate (figure 21). An orthotropic plate is a plate with different stiffnesses in perpendicular directions [11]. The plate moments m_{xx}, m_{yy}, m_{xy} and shear forces v_x, v_y are computed by a finite element program. When dimensioning the beams, the beam moments and beam shear force is calculated as follows.

$$M_x = m_{xx} b$$

$$M_t = -2 m_{xy} b$$

$$V = q_x b$$

In this, b is the centre to centre distance of the beams. The equations assume that the beams span in the x direction. Note the factor 2 in the formula for the torsion moment. The explanation is that the plate torsion moment m_{xy} occurs in two directions while the beam is in one direction.

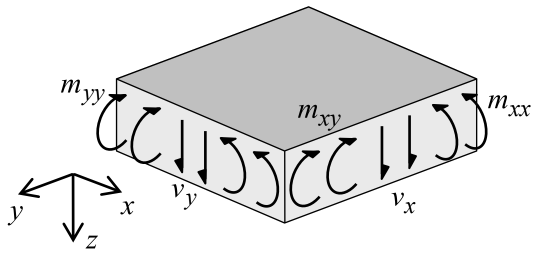

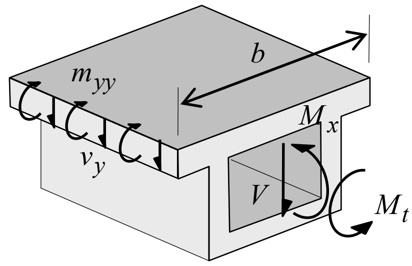

a Part of an orthotropic plate (idealisation) **b** Part of a beam (reality)
Figure 21. Moments and shear forces

The torsion stiffness of the orthotropic plate is $\frac{GI_t}{4b}$. (So $m_{xy} = \frac{GI_t}{4b} \rho_{xy}$.) In this GI_t is the torsion stiffness of a beam. The factor 4 is explained by the beam moment which is a factor 2 larger than the plate moment (see above) and the beam torsion deformation which is a factor 2 smaller than the definition of plate torsion deformation ($\rho_{xy} = -2 \frac{\partial^2 w}{\partial x \partial y}$).

By the way; an orthotropic plate model is not accurate. Deviations in moments and shear forces can be larger than 20%. Much more accurate is to model webs, top flanges and bottom flanges with plate elements too.

Example of a bridge deck

A cable stayed bridge has a deck of prestressed concrete (figure 22 and 23). The span between the pylons is l = 237.6 m. The I_t of the bridge deck cross section is calculated in the table below. Note that the cross beams (4) also contribute to the torsion stiffness of the deck. After all, they experience the same specific torsion as the other parts. You can convince yourself by twisting a sheet of paper: lines in both directions twist the same.

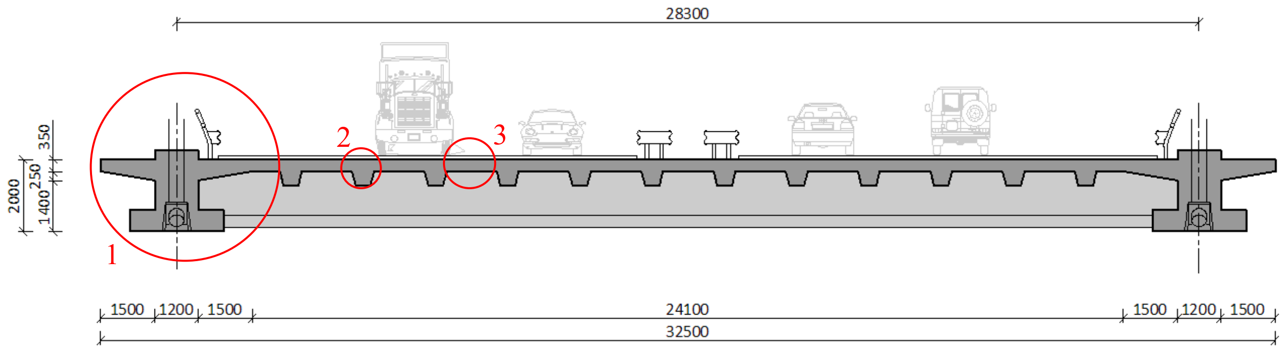

Figure 22. Cross section of the deck of a cable stayed bridge [12 p. 52]

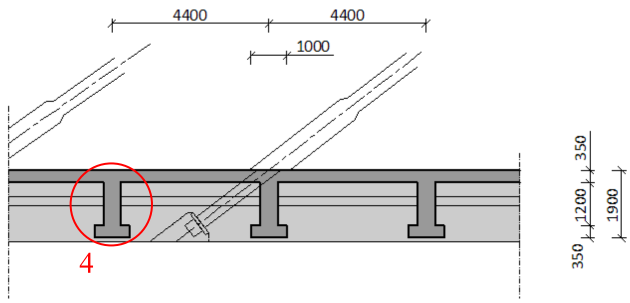

Figure 23. Longitudinal section of the deck of a cable stayed bridge [12]

i	I_{ti}	l_i	number	$I_{ti} \times l_i \times$ number / l	
1	1.0088 m^4	237.6 m	2	2.018 m^4	68 %
2	0.0232 m^4	4.4 m	12×54	0.279 m^4	10 %
3	0.0197 m^4	4.4 m	11×54	0.217 m^4	7 %
4	0.0696 m^4	28.3 m	53	0.439 m^4	15 %
			total I_t	2.950 m^4	100 %

Exercise, box

An open box is supported in 3 corners and loaded by a force in 1 corner. This load produces mostly torsion in the walls and bottom of the box. Show that the deflection is $u = \frac{3}{5} a^2 F \big/ G h^3$ and the shear stress is $\tau = \frac{3}{5} F \big/ h^2$. In this, h is de wall thickness. (This is not a simple exercise.)

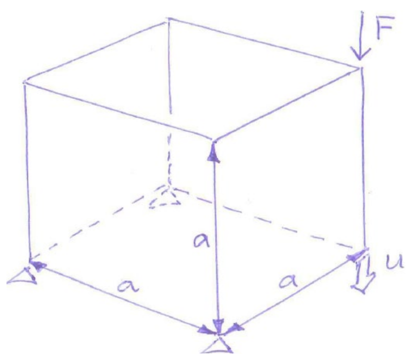

Local buckling

Thin wall tubes can buckle due to torsion. For example, the torsion moment at which a circular tubes buckles is

$$M_t = \frac{2\pi E\sqrt{r\,h^5}}{3\sqrt{2}(1-\nu^2)^{\frac{3}{4}}}.$$

In this, h is the wall thickness and r is the radius to the centre line of the wall [13].

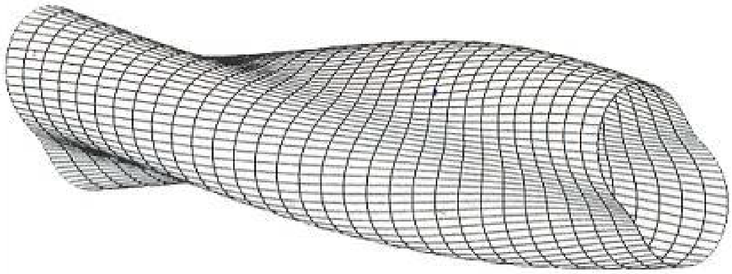

Figure 24. Buckling of a circular tube loaded in torsion

Volume elements

A beam can be also modelled with volume elements or solids. We can choose elements with 4, 8, 10 or 20 nodes. The 20 node elements are the best and these are considered here. The torsion stresses are computed with an error smaller than 3%, if we model 3 elements in the thickness (figure 25). The elements need to be approximately square in the cross section. This determines the number of elements in the beam depth. An error smaller than 1% is obtained with 5 elements in the thickness [14].

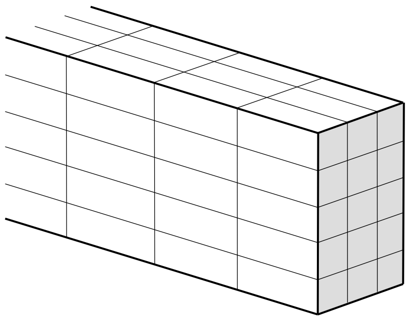

Figure 25: Element mesh for computing torsion stresses with an error smaller than 3%

Constrained warping

The typical torsion stresses only occur, if warping is not constrained (figure 26). In engineering practice this is often not the case. This causes deviations compared to the ideal torsion theory. The deviations occurs at supports, where torsion moments are applied and where the cross section changes.

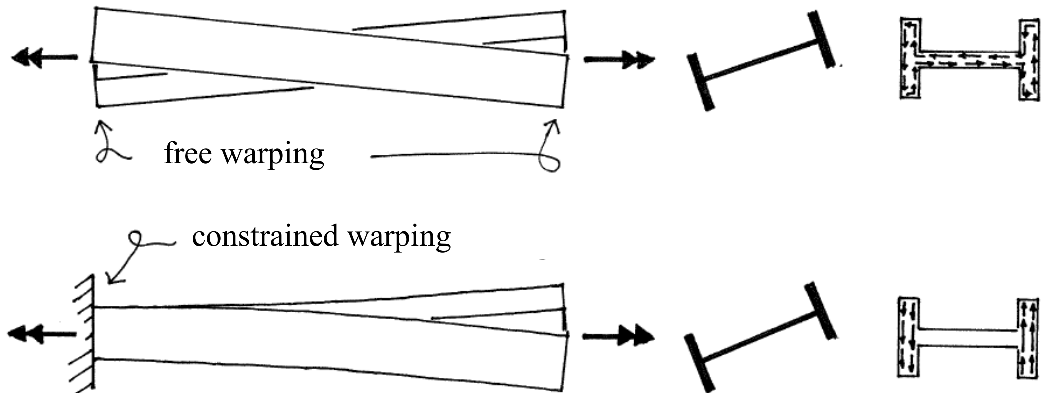

Figure 26. Torsion deformation of two short I sections

Especially thin wall open cross sections are sensitive to constrained warping. For example, in a cantilever I section, the theory of Saint-Venant is valid at a distance of approximately five times the section depth from the fixed end (figure 27).

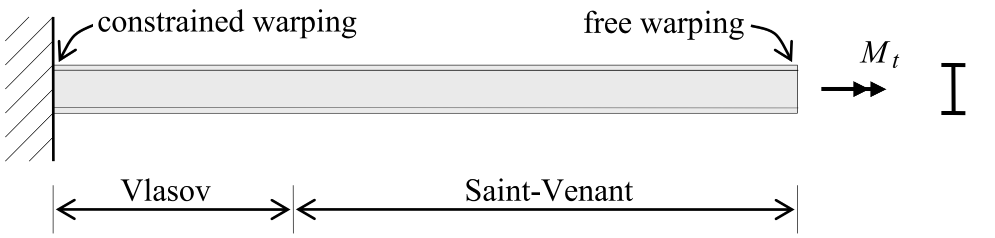

Figure 27. Influence of constrained warping

Theory by Vlasov [14]

In 1933, Vasiliy Vlasov developed a torsion theory which included constrained warping [15]. This theory is also called *warping torsion* or *non-uniform torsion*. Next to this, the torsion theory by Saint-Venant is also called *circulatory torsion* or *uniform torsion*. In Vlasov's theory the specific torsion deformation θ is not constant along the x axis. The cross section rotation $\varphi(x)$ follows from the differential equation

$$EC_w \frac{d^4\varphi}{dx^4} - GI_t \frac{d^2\varphi}{dx^2} = m_t .$$

In this, EC_w is the warping stiffness, GI_t is the torsion stiffness and m_t is a distributed torsion moment load along the beam. The warping constant C_w has the unit m^6 and is defined as

[14] Вла́сов Васи́лий Заха́рович (1906 – 1958) (Vasily Vlasov) was professor in Moscow. He wrote a book on thin wall beams (1940) for which he received the Stalin prize first class. He also wrote a book on shell structures (1949). [Russian Wikipedia]

$$C_w = \int_A \psi^2 dA \, .$$

The bi moment is defined as

$$B = -\int_A \sigma_{xx} \psi \, dA \, .$$

It occurs in a cross section when warping is constrained. It has the unusual unit Nm². When the differential equation is solved, the bi moment and the torsion moment can be calculated with

$$B = -EC_w \frac{d^2\varphi}{dx^2}$$
$$M_t = GI_t \frac{d\varphi}{dx} + \frac{dB}{dx}$$

(for a derivation see appendix 10). Vlasov's theory reduces to Saint-Venant's theory if the warping stiffness C_w is zero, the distributed moment load m_t is zero and warping is free.

Interpretation of the bi moment

For I sections the bi moment can be interpreted as the moment *M* in each of the flanges times their distance (figure 28)

$$B = M \, a \, .$$

This also explains the name (bi = 2). For other sections the interpretation is not this easy. Figure 28 shows that a bi moment occurs when warping is forced out of a cross section.

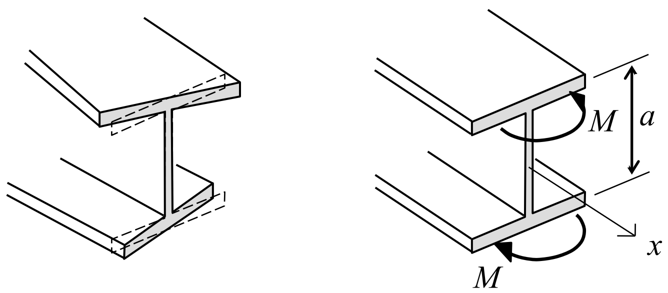

Figure 28. (left) Warping due to torsion and (right) the bi moment that removes this warping

Boundary conditions of the Vlasov theory

A beam end has an imposed rotation φ or an applied torsion moment M_t. We have to choose, one or the other. In addition, the beam end has an imposed warping $\frac{d\varphi}{dx}$ or an applied bi-moment *B*. Support examples are

fixed …………………………..	no rotation, no warping	$\varphi = 0$,	$\theta = 0$
fork support ……………………	no rotation, free warping	$\varphi = 0$,	$B = 0$
free end with a thick head plate ..	free rotation, no warping	$M_t = 0$,	$\theta = 0$
free end ………………………..	free rotation, free warping	$M_t = 0$,	$B = 0$

Example of a box girder bridge [15]

We consider a box girder bridge with a length $l = 60$ m. The torsion stiffness GI_t is $2690\ 10^8$ Nm^2 and the warping stiffness EC_w is $1183\ 10^9$ Nm^4. At both sides the bridge is supported without constraining warping. In the middle the bridge is supported by two temporary columns. One of these columns is knocked out in a construction accident. The remaining temporary column carries most of the bridge selfweight eccentrically. This introduces a very large torsion moment $T = 269\ 10^5$ Nm.

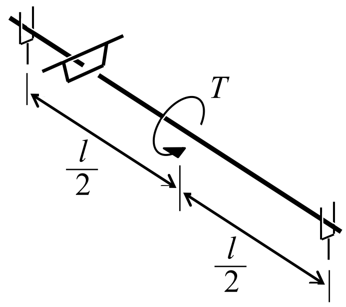

The boundary conditions at $x = 0$ and $x = l$ are

$$\varphi^- = 0 \qquad \frac{d^2\varphi^-}{dx^2} = 0 \qquad \varphi^+ = 0 \qquad \frac{d^2\varphi^+}{dx^2} = 0$$

The transition conditions in the middle $x = \frac{1}{2} l$ are

$$\varphi^- = \varphi^+ \qquad \frac{d\varphi^-}{dx} = \frac{d\varphi^+}{dx} \qquad \frac{d^2\varphi^-}{dx^2} = \frac{d^2\varphi^+}{dx^2}$$

$$GI_t \frac{d\varphi^-}{dx} - EC_w \frac{d^3\varphi^-}{dx^3} = T + GI_t \frac{d\varphi^+}{dx} - EC_w \frac{d^3\varphi^+}{dx^3}$$

The differential equation is solved by Maple (appendix 6) (figure 29, 30 and 31).

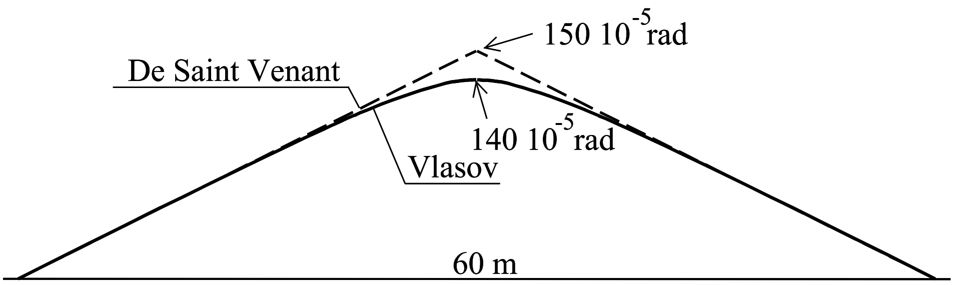

Figure 29. Cross section rotation φ

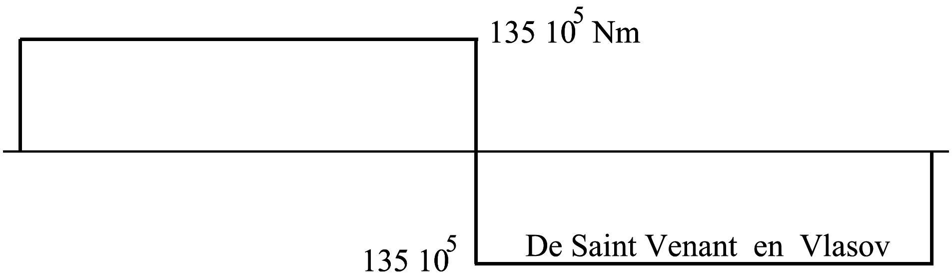

Figure 30. Torsion moment distribution M_t

[15] The situation is borrowed from a reader by Cor van der Veen [23], professor at Delft University of Technology.

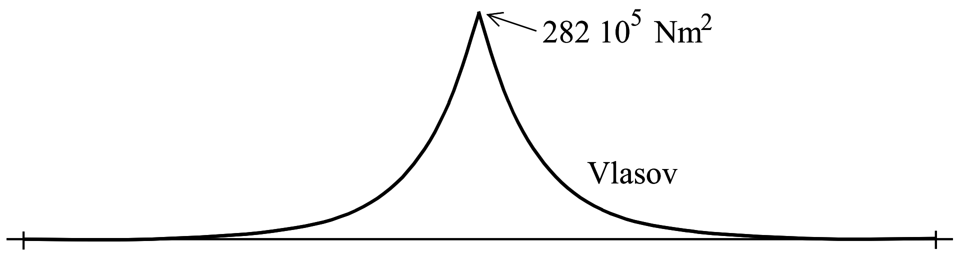

Figure 31. Bi moment distribution *B*

Interpretation of the moment distribution

The torsion moment distribution (figure 30) can be easily predicted. The torsion load can choose to go to the left support or the right support. It has a preference for the stiffest way. Both beam halves have the same stiffness (same length, same cross section). Therefore, half the torsion load goes to the left support and the other half goes to the right support.

Similarity with the shear force distribution

The torsion moment distribution in figure 30 has the shame shape as the shear force distribution due to a point load (not shown). Figure 32 shows another example. Since the torsion moment distribution looks like the shear force distribution they can be accidentally exchanged when studying finite element results. It is important to check this.

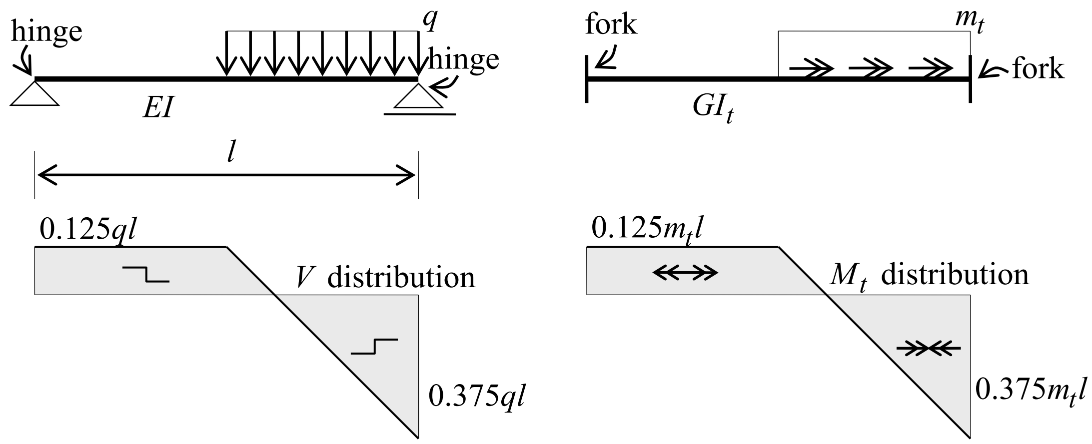

Figure 32. Similarity of shear force distribution and torsion moment distribution

Around the bend

In a complicated frame, it is not always clear where torsion moments come from. The following rules may be useful (figure 33).[16]

A bending moment that goes around the bend becomes a torsion moment.

A torsion moment that goes around the bend becomes a bending moment.

[16] Statement by Leo Wagemans, professor at Delft University of Technology.

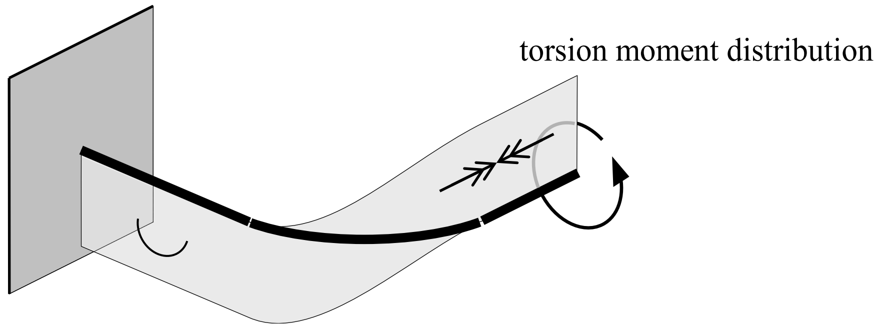

Figure 33. Moments in a curved beam

Head plate

A head plate that is welded to an I section constrains de warping according to the following equation.

$$B = \tfrac{1}{3} G t^3 b h \frac{d\varphi}{dx}$$

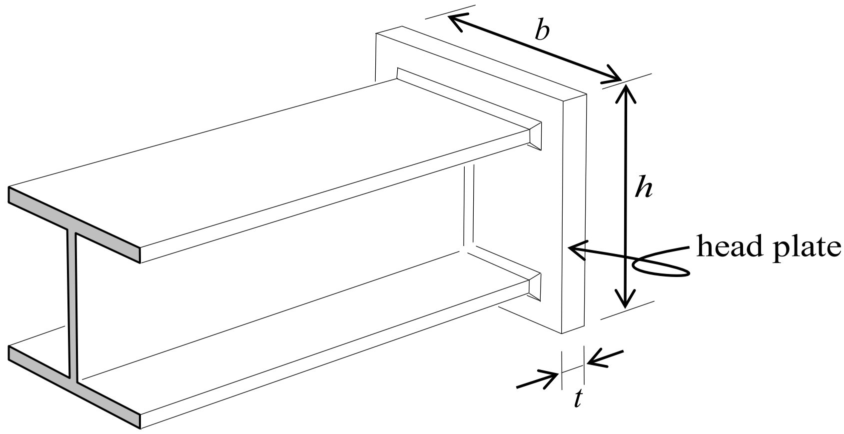

Figure 34. Head plate welded to an I section

Stresses according to Vlasov

The stress distribution according to the torsion theory of Vlasov consists of three parts.
1) shear stress according to the Saint-Venant theory
2) shear stress due to constrained warping
3) normal stress due to constrained warping

In general the largest values of the parts occur in different points of the cross section. Therefore software is needed to find the governing point. This is even more so if also stresses occur due to

4) normal force N
5) moment M_y in the y direction
6) moment M_z in the z direction

7) shear force V_y in the y direction

8) shear force V_z in de z direction

If y and z are the principal directions of the cross section, the normal stress are computed by [17]

$$\sigma_{xx}(y,z) = \frac{N}{A} + \frac{M_z}{I_{zz}} z + \frac{M_y}{I_{yy}} y - \frac{B}{C_w} \psi$$

Formulas also exist for shear stress in thin wall cross sections. However, these are too large to include here. As far as the author knows, there are no formulas for the shear stresses τ_{xy} and τ_{xz} due to constrained warping in solid cross sections.

Stresses in an I section

There is a simple formula for the largest normal stress in I sections due to a bi moment.

$$\sigma_{\max} = \frac{B}{\frac{1}{6}(h-t)\,t\,b^2}$$

In this, B is the bi moment, t is the flange thickness, b is the flange width and h is the cross section depth. The stress $\sigma_{\max}$ occurs in the edges of the flanges.

Example, stresses in a box girder bridge

We consider the box girder bridge of the previous example. The dimensions of the cross section are shown in figure 35. The program ShapeBuilder was used to compute the warping function ψ and the torsion properties of the cross section (figure 36). An extreme value of ψ is $-51100\,\text{cm}^2$ in the left bottom corner. Before, it was calculated that the largest bi moment is $B = 282\ \ 10^5\ \text{Nm}^2$ (figure 31). Therefore, the normal stress due to warping is

$$\sigma_{xx} = -\frac{B}{C_w}\psi = -\frac{282\ \ 10^5\,\text{Nm}^2}{39.44\ \text{m}^6}(-5.118\ \text{m}^2) = 3.66\ \ 10^6\ \text{N/m}^2 = 3.66\ \text{N/mm}^2$$

The reinforcement has a yield stress of 550 N/mm². The required reinforcement percentage is 3.66 / 550 = 0.7%. This is small despite the very large load. (Common reinforcement percentages are between 0.1 and 2.0%). Often, the stresses due to constrained warping are negligible for solid and closed cross sections. These stresses are not negligible in thin wall open cross sections.

[17] pronounce σ = sikma

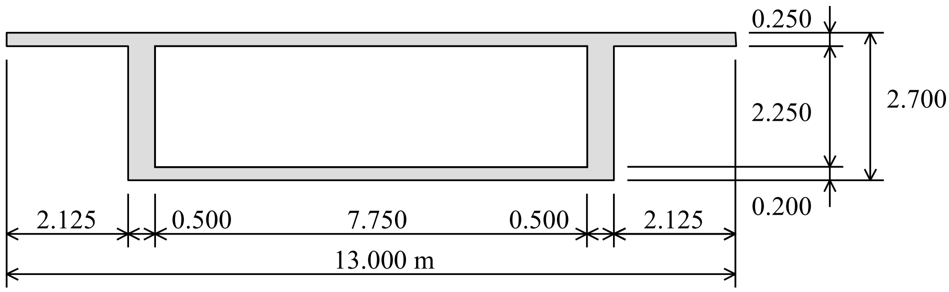

Figure 35. Cross section dimension of the box girder bridge

By the way, ShapeBuilder can compute all cross section properties, including shear stiffnesses, stress distribution due to shear forces and the location of the shear centre. To this end it solves similar differential equations as for torsion. This is not treated in this course.

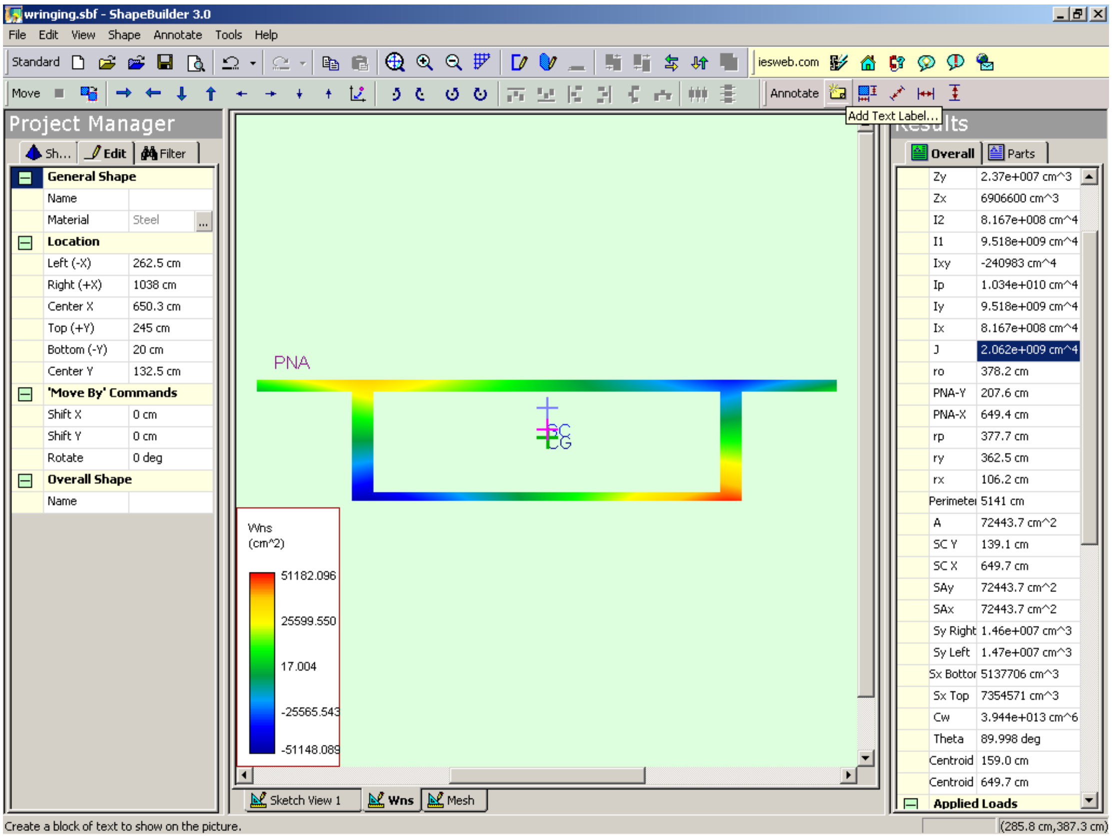

Figure 36. Warping function ψ of the box girder bridge

Distortion

The theories of Saint-Venant and Vlasov assume that a cross section warps but does not change shape in another way (See assumptions with figure 5). This is a good approximation for many beams. However, sometimes a cross section does change shape (figure 37). This is called distortion. To compute distortion we make a finite element model with shell elements.

Shell elements

Advantage of a computation with shell elements (figure 37) is that torsion and constrained warping are automatically included. The cross section properties GI_t, EC_w and the stresses τ_{max}, σ_{max} do not need to be calculated separately. Also, the model can be extended with diaphragms, support details and prestress cables. The computed stresses are more accurate than those computed with Saint-Venant or Vlasov. In addition, the model can be used to check global buckling and local buckling with a geometrically nonlinear computation.

Disadvantage of a computation with shell elements is that it is more work to build the model and cross section quantities such as torsion moments and shear forces are not readily available.

How to use shell elements is treated in a course on the finite element method for plates and disks.

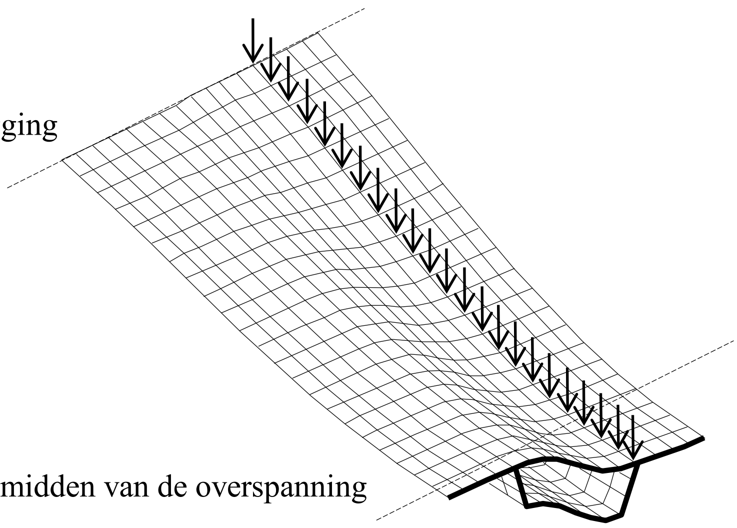

Figure 37. Distortion of a box girder bridge cross section [16]
(Half the bridge is drawn. The deformation is enlarged. Warping does not occur in the bridge middle.)

Example of a cantilever

We consider the cantilever of figure 38. The fixed end cannot warp. The other end is loaded by a torsion moment T while warping is free [17].

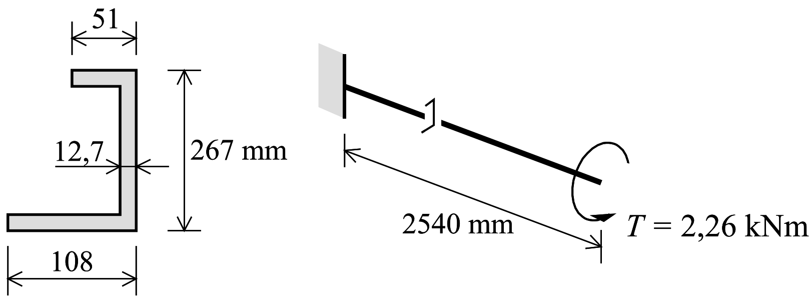

Figure 38. Cantilever

The material data and cross section data is
$E = 207000 \text{ N/mm}^2, G = 79300 \text{ N/mm}^2, \; I_w = 278000 \text{ mm}^4, \; C_w = 191 \; 10^8 \text{ mm}^6$.

The calculation is performed in appendix 7. Figure 39 shows the torsion moment distribution. At the support, the torsion moment is completely carried by constrained warping (Vlasov). At the free end, the torsion moment is completely carried by the shear flow in the cross section (Saint-Venant). Figure 40 shows the stresses in the fixed end and the free end.

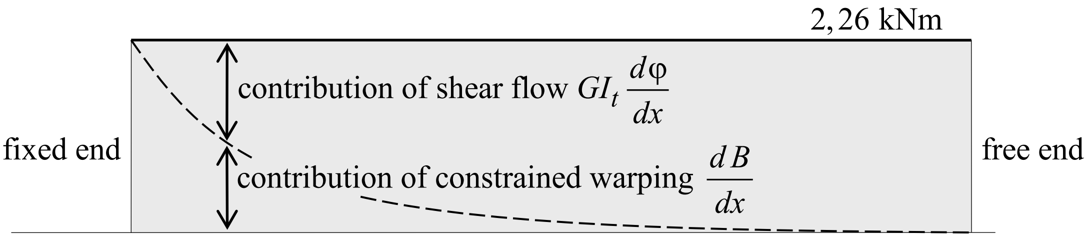

Figure 39. Torsion moment distribution M_t

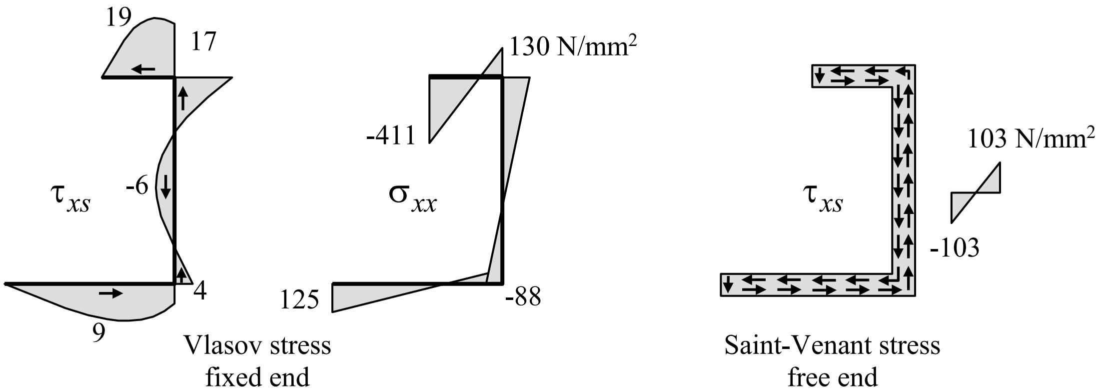

Figure 40. Stresses in cantilever cross sections [17]

Note that the largest Vlasov normal stress σ_{xx} is much larger than the Saint-Venant shear stress τ_{xs} (in absolute sense). The Vlasov shear stresses τ_{xs} are small, nonetheless, the moment they produce is equal to the load *T*.

Misunderstanding

It is a stubborn misunderstanding that for thin wall open cross sections the contribution of the torsion stiffness GI_t can be neglected. Table 3 shows the results of three computations. The first computation is the same as above; in the second computation the torsion stiffness GI_t is neglected and in the third computation the warping stiffness EC_w is neglected. The column with $\hat{\varphi}$ gives the rotations of the cantilever end. It is shown that EC_w cannot be neglected and GI_t can certainly not be neglected for computing the deformation of this beam.

Table 3. Consequences of neglecting stiffnesses

	GI_t	EC_w	$\hat{\varphi}$
1	$2,205 \cdot 10^{10}$ Nmm²	$3,954 \cdot 10^{15}$ Nmm⁴	$0,217$ rad
2	0	$3,954 \cdot 10^{15}$	3,180
3	$2,205 \cdot 10^{10}$	0	$0,260$

Future

All commercial frame analysis programs that the author knows, use Saint-Venant's theory and not Vlasov's. In the future, the programs can be extended with the Vlasov theory [18]. To that end, the section libraries need to contain not only the torsion constants I_t but also the warping constants C_w. The program user will be able to select whether the warping is constrained, free or linked for every beam end or column end. Linked means that two elements have the same warping where they are connected. Subsequently, the program will take this into account when computing the deformations and stresses. Appendix 9 gives the stiffness matrix of a frame element according to the Vlasov theory.

Characteristic length

The characteristic length is defined as

$$l_c = \sqrt{\frac{EC_w}{GI_t}}$$

This gives the length of the Vlasov part (figure 27). It is also a measure for the width of the peak in the bi moment distribution (figure 31): At a distance l_c from the constrained warping, the bi moment is 37% of its maximum value. At a distance of $3\,l_c$ is the bi-moment 5% of its maximum value.

Trick

All frame analysis programs make use of the torsion theory of Saint-Venant. We can use a trick to nonetheless include constrained warping [18]. When both ends of an element cannot warp, the torsion stiffness needs to be multiplied by the enlargement factor

$$\frac{l}{l - 2l_c}$$

where l is the beam length. When one of the beam ends cannot warp, the torsion stiffness needs to be multiplied by the enlargement factor

$$\frac{l}{l - l_c}.$$

Subsequently, the largest bi moment for both cases can be calculated by

$$\hat{B} \approx \pm\, l_c M_t \,.$$

Obviously, this occurs where the warping is constrained.[18] (The sign depends on the direction of the x axis of the element but actually the sign is not important.) The trick is valid if a distributed torsion moment is not present $m_x = 0$.
The trick is very accurate if $l \geq 6\,l_c$ (error < 1%). For smaller lengths, table 4 can be used.

Table 4. Magnification factors for torsion stiffness due to constrained warping [18]

beam length l	$0.5\,l_c$	$1\,l_c$	$1.5\,l_c$	$2\,l_c$	$2.5\,l_c$	$3\,l_c$	$4\,l_c$	$5\,l_c$
both sides constrained	49.2	13.2	6.53	4.19	3.11	2.52	1.93	1.65
one side constrained	13.2	4.19	2.52	1.93	1.65	1.50	1.33	1.25

The trick is useful to show that the real displacement due to torsion will be smaller than a common frame analysis predicts.

Safe or not safe?

Above it was shown that the real structure is stiffer than predicted by the Saint-Venant torsion theory. Consequently, real deformation will be smaller than computed deformations. So, for the serviceability limit state the common frame analysis is on the safe side.

Also it was shown that locally the real stresses can be much higher than predicted by the Saint-Venant torsion theory. However, this does not mean that the structural part will collapse. Most construction materials display somewhat plastic behaviour (aluminium, timber, reinforced concrete). According to plasticity theory, every equilibrium system with stresses smaller than or equal to the yield stress is a safe approximation for strength. A linear elastic computation according to the theory by Saint-Venant is such an equilibrium system. So, also for the ultimate limit state, the common frame analysis is on the safe side.

An exception is fatigue. In case of fatigue, the difference between the largest stress and the smallest stress in a material point is important. The largest stress is strongly reduced when the material yields at the first large load. However, the stress difference will not become smaller due to yielding and it occurs in every subsequent load. Therefore, in case of fatigue, choose circular tubes (these do not warp). If open section are necessary, it is important to let them warp freely. If nonetheless warping is constrained, warping stresses need to be accurately calculated and checked. Appendix 8 gives a calculation example.

The rule for constrained warping is: Prevention is better than calculating.

---

[18] The exact formula is

$$\hat{B} = \pm\, l_c M_t \tanh\frac{l}{2l_c} \quad \text{if both ends cannot warp}$$

$$\hat{B} = \pm\, l_c M_t \tanh\frac{l}{l_c} \quad \text{if one end cannot warp}$$

Torsional buckling and lateral torsional buckling

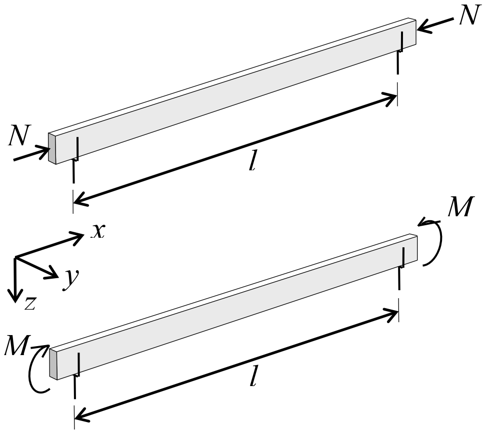

The quantities learned in this course can be also used in stability checks. The normal force at which a column fails in torsion buckling is

$$N = \frac{A}{I_p}\left(GI_t + \frac{\pi^2 EC_w}{l^2} \right).$$

The bending moment at which a beam fails in torsional lateral buckling is

$$M = \sqrt{\frac{\pi^2 EI_{yy}}{l^2}\left(GI_t + \frac{\pi^2 EC_w}{l^2} \right)}.$$

In this, l is the column or beam length and EI_{yy} is the bending stiffness in the lateral direction. These formulas are valid in the principal directions of a cross section and fork support at the ends [19].

Acknowledgement

Here, I like to thank Rene Braam, professor at Delft University of Technology, for his comments on the first edition.

Literature

1. K.N. Rahal, M.P. Collins, Effect of Thickness of Concrete Cover on Shear-Torsion Interaction – An Experimental Investigation, *ACI Structural Journal*, Vol. 92, No.3, 1995.
2. W.C. Young, *Roark's Formulas for Stress & Strain*, 6th edition, McGraw-Hill Book Company, New York, 1989.
3. A.J.C. Barré de Saint-Venant, Mémoire sur la torsion des prismes, *Mémoires présentés par divers savants a L'Académie des Sciences de L'Institut impérial de France et imprimés par son ordre: Sciences, Mathématiques et Physiques,* Volume 14, pp. 233-560, 1856.
4. J. Blaauwendraad, Theory of Elasticity, Reader, Delft University of Technology, October 2002.
5. S.P. Timoshenko, J.M. Gere, *Theory of Elastic Stability*, McGraw-Hill, New York, second edition 1961.
6. R. Bredt, Kritische Bemerkungen zur Drehungselastizität, *Zeitschrift der Vereines deutscher Ingenieure*, Vol. 40, No. 29. pp. 813-817, 1896.
7. L. Prandtl, Zur Torsion von prismatischen Stäben, *Physikalische Zeitschrift* 4, pp. 758-759, 1903.
8. W. Prager, Ph.G. Hodge, *Theory of Perfectly Plastic Solids*, Fourth Printing, John Wiley & Sons, New York 1965.
9. J.P. Den Hartog, *Advanced Strength of Materials*, McGraw-Hill, New York, 1952.
10. O.R. van der Meulen, Spanningsconcentratie door wringing, Bachelor-eindwerk, TU Delft, oktober 2005.
11. J. Blaauwendraad, *Plates and FEM*, Springer, 2010.
12. E. Bosman, Wind Induced Vibrations of frUHSC Bridge Decks, afstudeerverslag Technische Universiteit Delft, Faculteit Civiele Techniek, 2012.
13. M. Farshad, *Design and Analysis of Shell Structures*, Kluwer Academic Publishers, Dordrecht, 1992.
14. S.F. Landers, De nauwkeurigheid van wringspanningen berekend met de 3D eindige-elementenmethode, Bachelor Thesis, Delft University of Technology, October 2022, in Dutch, online: http://phoogenboom.nl/BSc_projects/eindrapport_landers.pdf
15. V.Z. Vlasov, *Thin-Walled Elastic Bars* (in Russian), 2nd ed., Fizmatgiz, Moscow, 1959.
16. G.A. Rombach, *Finite element design of concrete structures*, Thomas Telford Publishing, London, 2004.
17. W.F. Chen, T. Atsuta, *Theory of Beam-Columns*, *Vol. 2: Space Behaviour and Design*, McGraw-Hill, New York, 1977.
18. P.C.J. Hoogenboom, A. Borgart, Method for Including Constrained Warping in Traditional Frame Analyses, *HERON*, Vol. 50 No. 1 pp. 55-68, 2005
19. H. de Jong, Instabiliteit, Kip, torsieknik en plooien, Hoofdstuk 2 van het dictaat g12N Staalconstructies II, TU Delft, 1988.
20. P.C.J. Hoogenboom, Theory of Elasticity, Exam Problems and Answers, reader, Delft University of Technology, November 2002, online: phoogenboom.nl/b16_exam_ problems.pdf (retrieved 16 Jan. 2023)
21. R.W. Clough, E.L. Wilson, Early finite element research at Berkeley, Fifth US national conference on computational mechanics, 4-6 August 1999, online: https://www.smart-fem.de/media/fe-history.pdf
22. K. E. Kurrer, Rudolph Bredt. Zum 100. Todestag des Altmeisters des deutschen Kranbaus, *Stahlbau*, 2013

23. C. van der Veen, Design Concrete Bridges, dictaat TU Delft, 2017.

Appendix 1. Formulas for torsion properties [2, table 20]

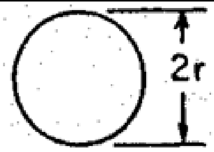	$I_t = \frac{1}{2}\pi r^4$ $\tau_{\max} = \dfrac{M_t}{\frac{1}{2}\pi r^3}$
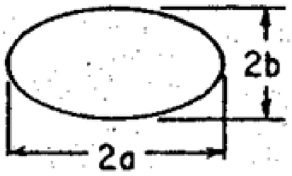	$I_t = \dfrac{\pi a^3 b^3}{a^2 + b^2}$ $\tau_{\max} = \dfrac{M_t}{\frac{1}{2}\pi a b^2}$
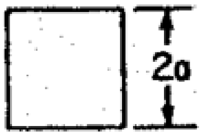	$I_t = 2.25 a^4$ $\tau_{\max} = \dfrac{M_t}{1.66 a^3}$
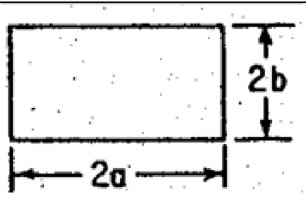	$I_t = ab^3\left(\frac{16}{3} - 3.36\dfrac{b}{a}(1 - \frac{1}{12}\dfrac{b^4}{a^4})\right) \qquad a \ge b$ $\tau_{\max} = \dfrac{3M_t}{8ab^2}\left(1 + 0.6095\dfrac{b}{a} + 0.8865\dfrac{b^2}{a^2} - 1.8023\dfrac{b^3}{a^3} + 0.9100\dfrac{b^4}{a^4}\right)$
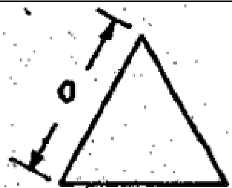	$I_t = \frac{1}{80}\sqrt{3}\, a^4$ $\tau_{\max} = \dfrac{M_t}{\frac{1}{20} a^3}$
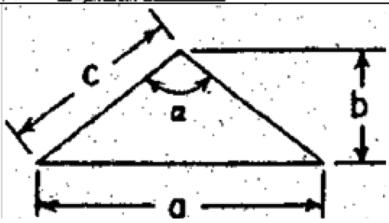	$I_t = \dfrac{a^3 b^3}{15a^2 + 20b^2} \qquad \frac{2}{3} < \dfrac{a}{b} < \sqrt{3}$ $I_t = 0.0915 b^4\left(\dfrac{a}{b} - 0.8592\right) \qquad \sqrt{3} < \dfrac{a}{b} < 2\sqrt{3}$ $\tau_{\max} = \dfrac{M_t\, b\left(0.200 + 0.309\dfrac{a}{b} - 0.0418\dfrac{a^2}{b^2}\right)}{I_t} \qquad \frac{2}{3} < \dfrac{a}{b} < 2\sqrt{3}$
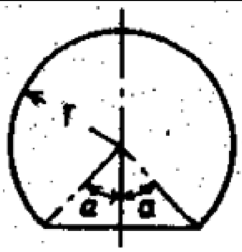 $h = r(1 - \cos\alpha)$	$I_t = 2r^4\left(0.7854 - 0.0333\dfrac{h}{r} - 2.6183\dfrac{h^2}{r^2} + 4.1595\dfrac{h^3}{r^3} - 3.0769\dfrac{h^4}{r^4} + 0.9299\dfrac{h^5}{r^5}\right)$ $\tau_{\max} = \dfrac{M_t}{r^3}\left(0.6366 + 1.7598\dfrac{h}{r} - 5.4897\dfrac{h^2}{r^2} + 14.062\dfrac{h^3}{r^3} - 14.510\dfrac{h^4}{r^4} + 6.434\dfrac{h^5}{r^5}\right)$ $0 \le \dfrac{h}{r} \le 1$

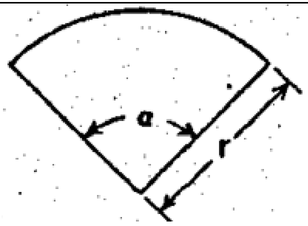	$I_t = r^4\left(0.0034 - 0.0697\frac{\alpha}{\pi} + 0.5825\frac{\alpha^2}{\pi^2} - 0.2950\frac{\alpha^3}{\pi^3} + 0.0874\frac{\alpha^4}{\pi^4} - 0.0111\frac{\alpha^5}{\pi^5}\right)$ $0.1 \le \frac{\alpha}{\pi} \le 2.0$ $\tau_{\max} = \frac{M_t}{r^3\left(0.0117 - 0.2137\frac{\alpha}{\pi} + 2.2475\frac{\alpha^2}{\pi^2} - 4.6709\frac{\alpha^3}{\pi^3} + 5.1764\frac{\alpha^4}{\pi^4} - 2.2000\frac{\alpha^5}{\pi^5}\right)}$ $0.1 \le \frac{\alpha}{\pi} \le 1.0$
two flat sides 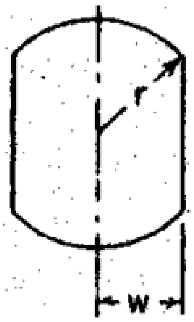 $h = r - w$	$I_t = 2r^4\left(0.7854 - 0.4053\frac{h}{r} - 3.5810\frac{h^2}{r^2} + 5.2708\frac{h^3}{r^3} - 2.0772\frac{h^4}{r^4}\right)$ $0 \le \frac{h}{r} \le 0.8$ $\tau_{\max} = \frac{M_t}{r^3}\left(0.6366 + 2.5303\frac{h}{r} - 11.157\frac{h^2}{r^2} + 49.568\frac{h^3}{r^3} - 85.886\frac{h^4}{r^4} + 69.849\frac{h^5}{r^5}\right)$ $0 \le \frac{h}{r} \le 0.6$
four flat sides $h = r - w$	$I_t = 2r^4\left(0.7854 - 0.7000\frac{h}{r} - 7.7982\frac{h^2}{r^2} + 14.578\frac{h^3}{r^3}\right)$ $\tau_{\max} = \frac{M_t}{r^3}\left(0.6366 + 2.6298\frac{h}{r} - 5.6147\frac{h^2}{r^2} + 30.853\frac{h^3}{r^3}\right)$ $0 \le \frac{h}{r} \le 0.293$
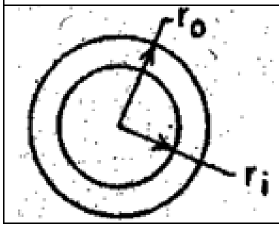	$I_t = \frac{1}{2}\pi(r_o^4 - r_i^4)$ $\tau_{\max} = \frac{r_o M_t}{\frac{1}{2}\pi(r_o^4 - r_i^4)}$

<table>
<tr>
<td>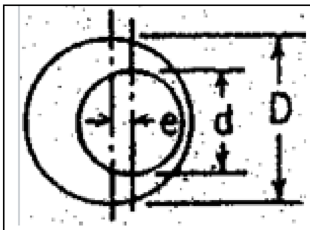
$\lambda = \frac{e}{D}$
$n = \frac{d}{D}$</td>
<td>$$I_t = \frac{\pi(D^4 - d^4)}{32\left(1 + \frac{16n^2}{(1-n^2)(1-n^4)}\lambda^2 + \frac{384n^4}{(1-n^2)^2(1-n^4)^4}\lambda^4\right)}$$
$$\tau_{\max} = \frac{16DM_t}{\pi(D^4 - d^4)}\left(1 + \frac{4n^2}{1-n^2}\lambda + \frac{32n^2}{(1-n^2)(1-n^4)}\lambda^2 + \frac{48n^2(1+2n^2+3n^4+2n^6)}{(1-n^2)(1-n^4)(1-n^6)}\lambda^3 + \frac{64n^2(2+12n^2+19n^4+28n^6+18n^8+14n^{10}+3n^{12})}{(1-n^2)(1-n^4)(1-n^6)(1-n^8)}\lambda^4\right)$$</td>
</tr>
<tr>
<td>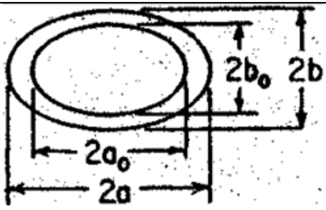
thickness not constant</td>
<td>$$I_t = \frac{\pi a^3 b^3}{a^2 + b^2}(1 - q^4)$$
$$\tau_{\max} = \frac{M_t}{\frac{1}{2}\pi a b^2 (1 - q^4)}$$
$$q = \frac{a_o}{a} = \frac{b_o}{b}$$</td>
</tr>
<tr>
<td>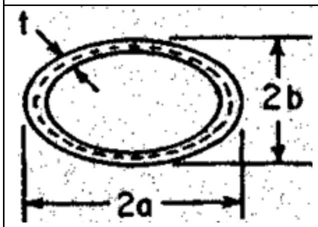
constant thickness</td>
<td>$$I_t = \frac{4\pi^2 t (a - \frac{1}{2}t)^2 (b - \frac{1}{2}t)^2}{\pi(a+b-t)\left(1 + 0.258\frac{(a-b)^2}{(a+b-t)^2}\right)}$$
$$\tau_{\text{average}} = \frac{M_t}{2\pi t (a - \frac{1}{2}t)(b - \frac{1}{2}t)}$$</td>
</tr>
<tr>
<td>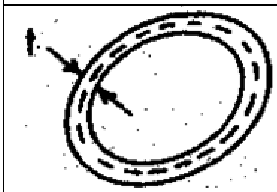
constante thickness</td>
<td>$$I_t = \frac{4A^2 t}{U}$$
$$\tau_{\text{average}} = \frac{M_t}{2At}$$
A is the average of the surfaces enclosed by the outer edge and inner edge.
U is the length of the median edge</td>
</tr>
<tr>
<td>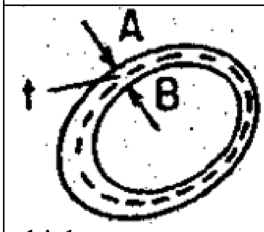
thickness not constant</td>
<td>$$I_t = \frac{4A^2}{\int \frac{1}{t}\, dU}$$
$$\tau_{\text{average}} = \frac{M_t}{2At}$$</td>
</tr>
</table>

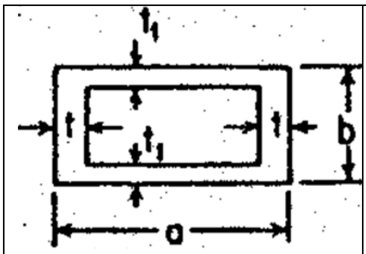	$I_t = \frac{2 t t_1 (a-t)^2 (b-t_1)^2}{t(a-t)+t_1(b-t_1)}$ $\quad t, t_1 \ll a, b$ $\tau_{\text{average}} = \frac{M_t}{2t(a-t)(b-t_1)}$ in the short sides $\tau_{\text{average}} = \frac{M_t}{2t_1(a-t)(b-t_1)}$ in the long sides There will be higher stresses in inner corners unless fillets of fairly large radius are provided
 constant thickness	$I_t = \frac{2}{3}\pi r t^3$ $\tau_{\max} = \frac{(6\pi r + 1.8t)M_t}{4\pi^2 r^2 t^2}$ $t \ll r$
 constant thickness	$I_t = \frac{1}{3} U t^3$ $\tau_{\max} = \frac{(3U + 1.8t)M_t}{U^2 t^2}$ $t \ll r$ U is the lengte of the median line
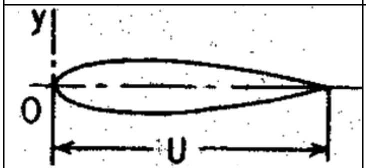	$I_t = \frac{1}{\frac{1}{4I_x} + \frac{4}{AU^2}}$ $\tau = \frac{M_t D}{I_t} \frac{1 + 0.15\left(\frac{\pi^2 D^4}{16A^2} - \frac{D}{2r}\right)}{1 + \frac{\pi^2 D^4}{16A^2}}$ I_x is the moment of inertia around the x axis. A is the cross-section area. D is the diameter of the largest inscribed circle. r is the radius of curvature of the boundary at the location of the stress.
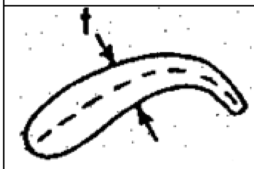	$I_t = \frac{1}{\frac{3}{F} + \frac{4}{AU^2}}$ $\quad F = \int_0^U t^3 dU$ A is the cross-section area. U is the length of the dashed median line. τ as in previous cross-section.
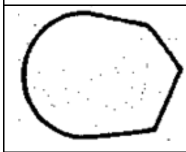	$I_t = \frac{A^4}{40 I_p}$ τ as in previous cross-section.

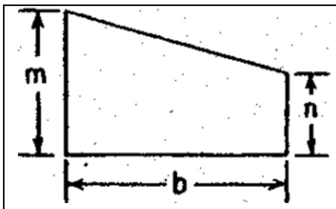	$I_t = \frac{1}{12} b(m+n)(m^2+n^2) -$ $- m^4\left(0.10504 - 0.10s + 0.0848s^2 - 0.06746s^3 + 0.0515s^4\right) -$ $- n^4\left(0.10504 + 0.10s + 0.0848s^2 + 0.06746s^3 + 0.0515s^4\right)$ $s = \frac{m-n}{b}$ $\tau = \frac{M_t D}{I_t} \frac{1}{1+\frac{\pi^2 D^4}{16A^2}}$
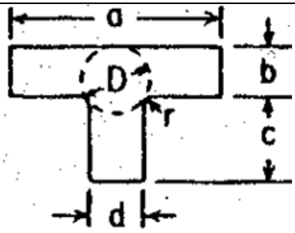	$I_t = ab^3\left(\frac{1}{3} - 0.21\frac{b}{a}(1-\frac{b^4}{12a^4})\right) + cd^3\left(\frac{1}{3} - 0.105\frac{d}{c}(1-\frac{d^4}{192c^4})\right) +$ $+ D^4\left(0.15 + 0.10\frac{r}{b}\right)\min(\frac{b}{d},\frac{d}{b})$ $D = \frac{(b+r)^2 + rd + \frac{1}{4}d^2}{2r+b} \qquad d < 2(b+r)$ $\tau = \frac{M_t D}{I_t} \frac{1 + 0.0899\ln(1+\frac{D}{2r}) + 0.181\frac{D}{2r}}{1+\frac{\pi^2 D^4}{16A^2}}$
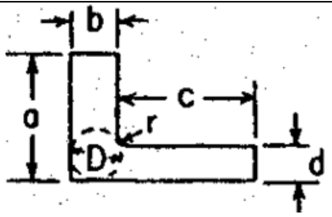	$I_t = ab^3\left(\frac{1}{3} - 0.21\frac{b}{a}(1-\frac{b^4}{12a^4})\right) + cd^3\left(\frac{1}{3} - 0.105\frac{d}{c}(1-\frac{d^4}{192c^4})\right) +$ $+ D^4\frac{d}{b}\left(0.07 + 0.076\frac{r}{b}\right)$ $D = 2\left(d + b + 3r - \sqrt{2(2r+b)(2r+d)}\right) \qquad d \le b < 2(d+r)$ τ as in previous cross-section
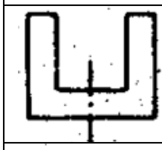 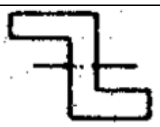	As previous cross-section (sum of the parts)
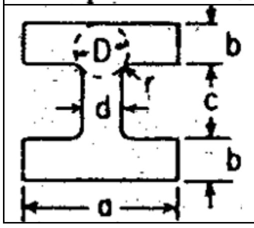	$I_t = 2ab^3\left(\frac{1}{3} - 0.21\frac{b}{a}(1-\frac{b^4}{12a^4})\right) + \frac{1}{3}cd^3 + 2D^4\left(0.15 + 0.10\frac{r}{b}\right)\min(\frac{b}{d},\frac{d}{b})$ τ as in previous cross-section

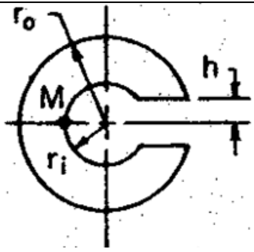	$I_t = 2r_o^4\left(k_1 + k_2\frac{r_i}{r_o} + k_3\frac{r_i^2}{r_o^2} + k_4\frac{r_i^3}{r_o^3}\right)$ $\tau_{max} = \frac{M_t}{r_o^3}\left(h_1 + h_2\frac{r_i}{r_o} + h_3\frac{r_i^2}{r_o^2} + h_4\frac{r_i^3}{r_o^3}\right)$ $k_1 = 0.4427 + 0.0064\frac{h}{r_i} - 0.0201\frac{h^2}{r_i^2}$ $h_1 = 2.0014 - 0.1400\frac{h}{r_i} - 0.3231\frac{h^2}{r_i^2}$ $k_2 = -0.8071 - 0.4047\frac{h}{r_i} + 0.1051\frac{h^2}{r_i^2}$ $h_2 = 2.9047 + 3.0069\frac{h}{r_i} + 4.0500\frac{h^2}{r_i^2}$ $k_3 = -0.0469 + 1.2063\frac{h}{r_i} - 0.3538\frac{h^2}{r_i^2}$ $h_3 = -15.721 - 6.5077\frac{h}{r_i} - 12.496\frac{h^2}{r_i^2}$ $k_4 = 0.5023 - 0.9618\frac{h}{r_i} + 0.3639\frac{h^2}{r_i^2}$ $h_4 = 29.553 + 4.1115\frac{h}{r_i} + 18.845\frac{h^2}{r_i^2}$ $0.2 \le \frac{r_i}{r_o} \le 0.6$ $0.1 \le \frac{h}{r_i} \le 1.0$
In Roark's [2] are torsion formulas for 8 more cross sections of machine axis.	

Appendix 2. Calculation of the torsion properties of a multi-cell box girder

[4, Volume 1, p. 196]

In this example the torsion stiffness and shear stresses are calculated of a multi-cell box girder bridge (figure 41). The thickness of the top deck ($t/2$) is half the thickness (t) of the other parts. Since $t \ll a$, we can work with the centre-to-centre distances (a and $2a$) of the box walls. The contributions of the walls themselves can be also neglected. The cantilever flanges of the box can be neglected for the same reason.

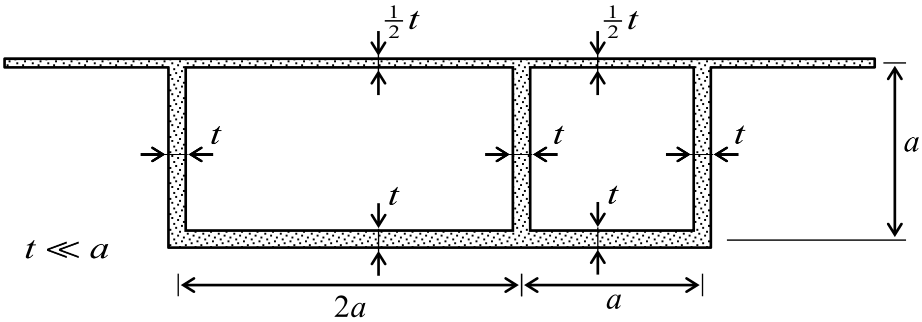

Figure 41. Cross section of the bridge

Figure 42 shows the cross section, the soap film and two weightless plates that occur in the membrane analogy. The left plate moves w_1 and the right plate moves w_2. In this drawing we choose w_2 larger than w_1 . This will be consistently used in the calculation. The answers will show whether the assumption was correct.

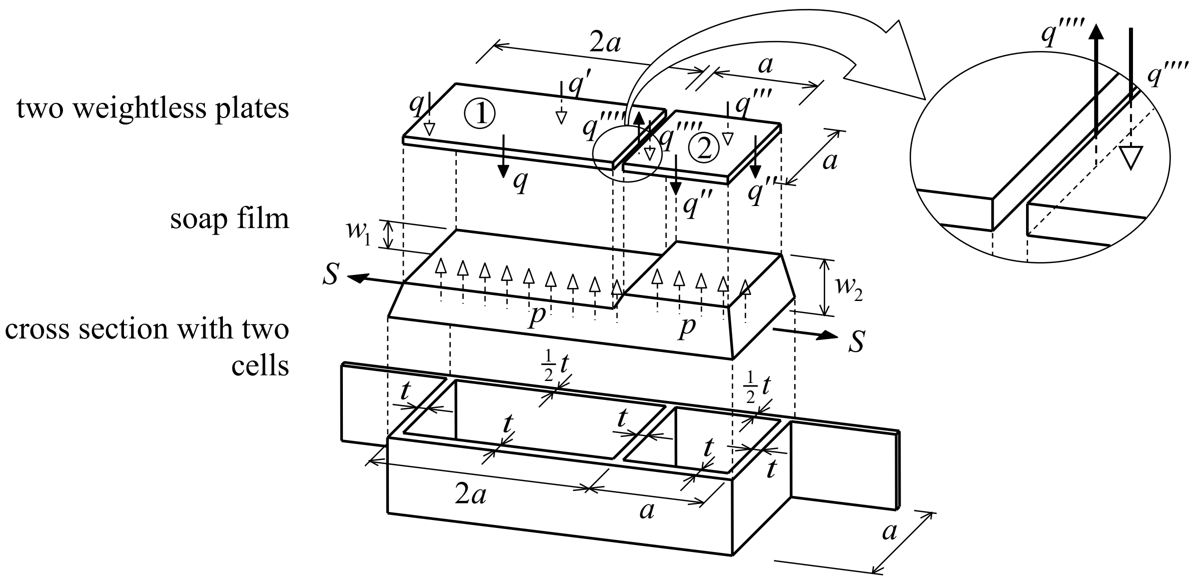

Figure 42. Equilibrium of soap film and weightless plates

The soap film membrane shear forces q play a large part in the calculation. Since w_2 is larger than w_1 , the drawn shear forces will have positive values.

$$q = \frac{w_1}{t} S \qquad q' = \frac{w_1}{\frac{1}{2}t} S \qquad q'' = \frac{w_2}{t} S \qquad q''' = \frac{w_2}{\frac{1}{2}t} S \qquad q'''' = \frac{w_2 - w_1}{t} S$$

The first four shear forces q, q', q'' and q''' act downwards on the plates. The last shear force q'''' acts up on plate 1 and down on plate 2 (If w_1 were larger than w_2 , this would be the other way around). The vertical equilibrium is

$$\begin{aligned} &q\,a \;+ q\,2a \;+\; q'\,2a \;-\; q''''\,a \;=\; p\,2a\,a \qquad (\textit{plate}\ 1) \\ &q''\,a \;+\; q''\,a \;+\; q'''\,a \;+\; q''''\,a \;=\; p\,a\,a \qquad (\textit{plate}\ 2) \end{aligned}$$

So

$$\begin{aligned} &\frac{w_1}{t}S\,a \;+\; \frac{w_1}{t}S\,2a \;+\; \frac{w_1}{\frac{1}{2}t}S\,2a \;-\; \frac{w_2 - w_1}{t}S\,a \;=\; 2p\,a^2 \qquad (\textit{plate}\ 1) \\ &\frac{w_2}{t}S\,a \;+\; \frac{w_2}{t}S\,a \;+\; \frac{w_2}{\frac{1}{2}t}S\,a \;+\; \frac{w_2 - w_1}{t}S\,a \;=\; p\,a^2 \qquad (\textit{plate}\ 2) \end{aligned}$$

Simplified and divided by a

$$\begin{aligned} &8\frac{S}{t}w_1 \;-\; \frac{S}{t}w_2 \;=\; 2p\,a \qquad (\textit{plate}\ 1) \\ &-\frac{S}{t}w_1 \;+\; 5\frac{S}{t}w_2 \;=\; p\,a \qquad (\textit{plate}\ 2) \end{aligned}$$

From these two equations we solve

$$w_1 = \frac{11}{39}\frac{p}{S}a\,t \qquad w_2 = \frac{10}{39}\frac{p}{S}a\,t$$

The displacement w_2 is smaller than w_1. So, in fact, shear force q'''' acts opposite to what is drawn.

We make the transition to the ϕ –hill with $w = \phi$, $p = 2\theta$ and $S = 1/G$. The result is

$$\phi_1 = \frac{22}{39}G\,a\,t\,\theta \qquad \phi_2 = \frac{20}{39}G\,a\,t\,\theta$$

The torsion moment is twice the volume of the ϕ –hill

$$M_t = 2(\phi_1 \cdot 2a \cdot a + \phi_2 \cdot a \cdot a) \;\;\rightarrow\;\; M_t = \frac{128}{39}G\,a^3\,t\,\theta$$

Apparently, the torsion constant is

$$I_t = \frac{128}{39}a^3\,t$$

We express ϕ_1 and ϕ_2 in the moment

$$\phi_1 = \frac{11}{64}\frac{M_t}{a^2} \qquad \phi_2 = \frac{10}{64}\frac{M_t}{a^2}$$

The stresses we calculate from the slope of the ϕ –hill (figure 43)

$$\tau = \frac{\phi_1}{t} = \frac{11}{64}\frac{M_t}{ta^2} \qquad \tau' = \frac{\phi_1}{\frac{1}{2}t} = \frac{22}{64}\frac{M_t}{ta^2} \qquad \tau'' = \frac{\phi_2}{t} = \frac{10}{64}\frac{M_t}{ta^2}$$

$$\tau''' = \frac{\phi_2}{\frac{1}{2}t} = \frac{20}{64}\frac{M_t}{ta^2} \qquad \tau'''' = \frac{\phi_1 - \phi_2}{t} = \frac{1}{64}\frac{M_t}{ta^2}$$

Figure 43 shows the true directions of the shear stresses. The direction of the first arrow can be chosen and the other arrow directions follow from the ϕ –hill slopes. The middle web has the same slope as the right hand web, consequently, τ'''' has the same direction as τ''.

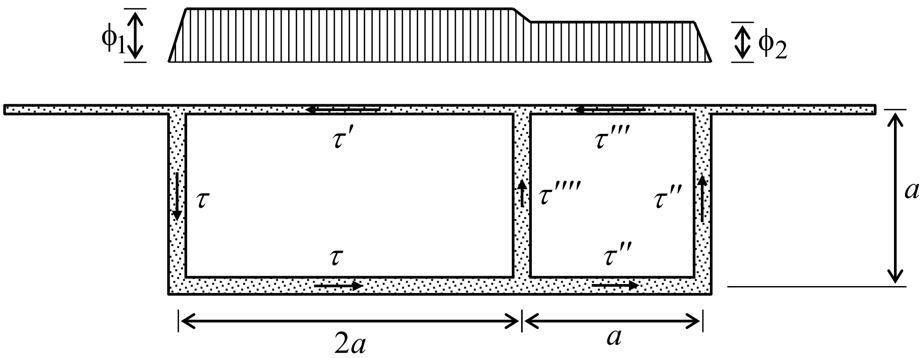

Figure 43. Shear stresses in the cross section

Exercises

The resultant of the vertical shear stresses should be zero. The resultant of the horizontal shear stresses should be zero. Check this.

The vertical shear stresses should give a torsion moment $\frac{1}{2}M_t$. The horizontal shear stresses should give a torsion moment $\frac{1}{2}M_t$. Check this.

Use Bredt's formulas to calculate torsion constant I_t and the stresses τ, if the middle web is left out. What do you conclude?

Appendix 3. Calculation of a nabla girder

The prestressed concrete box girder of this example is known in the Netherlands as nabla girder applied in the Deltawerken when closing the Haringvliet. What follows is a Delft University exam problem (Elasticity theory, 12 Jan. 1998) [20].

A box girder is loaded in torsion. The thickness of all walls is h (see figure). We calculate the girder with the membrane analogy. The weightless plates in the corners of the girder will have the same displacement because the girder is rotation symmetrical.

a Calculate the displacements w_1 and w_2 of the weightless plates.

b Calculate the torsion stiffness GI_t of the cross section.

c Calculate the shear stresses in the cross section and draw them in the correct directions.

d Suppose that warping in the girder is locally constrained. Will this increase the torsion stiffness, or will it become smaller, or will it stay the same? Explain your answer.

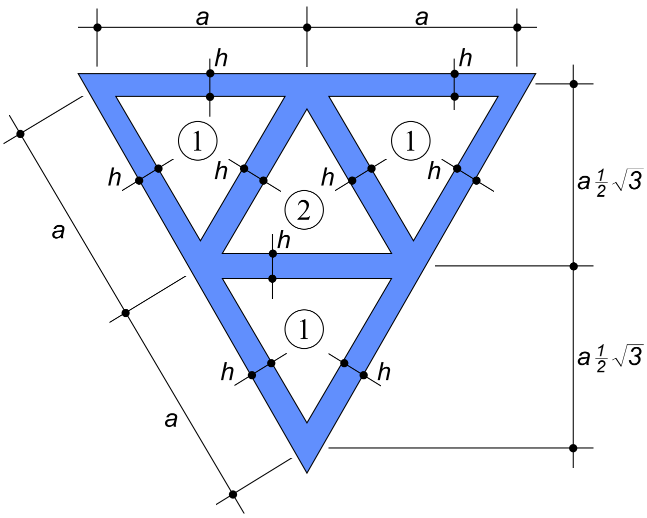

Answers

a <u>Weightless plates</u>

We choose w_2 of the middle cell larger than w_1 of the corner cells. Equilibrium of the weightless plate above the corner cells is

$$p\frac{1}{2}a\,a\frac{1}{2}\sqrt{3} = a\,S\frac{w_1}{h} + a\,S\frac{w_1}{h} - a\,S\frac{w_2 - w_1}{h}$$

Equilibrium of the weightless plate above the middle cell gives

$$p\frac{1}{2}a\,a\frac{1}{2}\sqrt{3} = a\,S\frac{w_2 - w_1}{h} + a\,S\frac{w_2 - w_1}{h} + a\,S\frac{w_2 - w_1}{h}$$

This can be simplified to

$$p\tfrac{1}{4}a\sqrt{3}=\frac{S}{h}(3\,w_1-w_2)$$
$$p\tfrac{1}{4}a\sqrt{3}=\frac{S}{h}3\,(w_2-w_1)$$

from which we can solve w_1 and w_2 .

$$\boxed{\begin{aligned} w_1&=\tfrac{1}{6}\sqrt{3}\,\frac{p}{S}ah \\ w_2&=\tfrac{1}{4}\sqrt{3}\,\frac{p}{S}ah \end{aligned}}$$

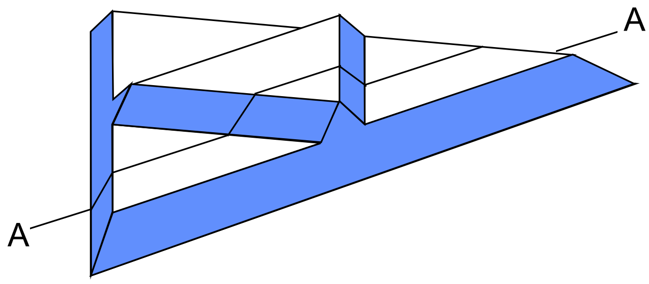

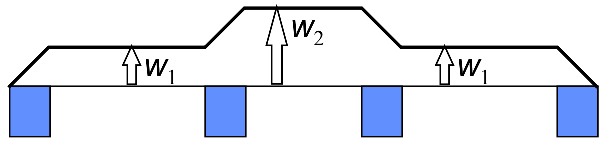

cross section A-A

b <u>Torsion stiffness</u>

From the soap film we go to the ϕ – hill with the following substitutions.

$$w=\phi$$
$$p=2\theta$$
$$S=\frac{1}{G}$$

So

$$\phi_1=\tfrac{1}{3}\sqrt{3}\,\theta G\,ah$$
$$\phi_2=\tfrac{1}{2}\sqrt{3}\,\theta G\,ah$$

The torsion moment is two times the volume of the ϕ –hill.

$$\begin{aligned} M_t &= 2\left(\tfrac{1}{2}a\,a\tfrac{1}{2}\sqrt{3}\,\phi_1+\tfrac{1}{2}a\,a\tfrac{1}{2}\sqrt{3}\,\phi_1+\tfrac{1}{2}a\,a\tfrac{1}{2}\sqrt{3}\,\phi_1+\tfrac{1}{2}a\,a\tfrac{1}{2}\sqrt{3}\,\phi_2\right) \\ &= a^2\tfrac{1}{2}\sqrt{3}\,(3\,\phi_1+\phi_2) \end{aligned}$$

Substitution of the former in the latter gives

$$\begin{aligned} M_t &= a^2\,\tfrac{1}{2}\sqrt{3}\left(3\,\tfrac{1}{3}\sqrt{3}\,\theta G\,ah+\tfrac{1}{2}\sqrt{3}\,\theta G\,ah\right) \\ &= a^2\,\tfrac{1}{2}3(1+\tfrac{1}{2})\,\theta G\,ah \\ &= G\,\tfrac{9}{4}\,a^3h\;\;\theta \end{aligned}$$

For a beam model of the girder holds

$$M_t=GI_t\,\theta$$

So, the torsion stiffness is

$$\boxed{GI_t = G\tfrac{9}{4}a^3 h}$$

c Shear stress

The shear stress is the slope of the ϕ –hill. First, we rewrite the equation for the torsion moment

$$\theta G\,ah = \tfrac{4}{9}\frac{M_t}{a^2}$$

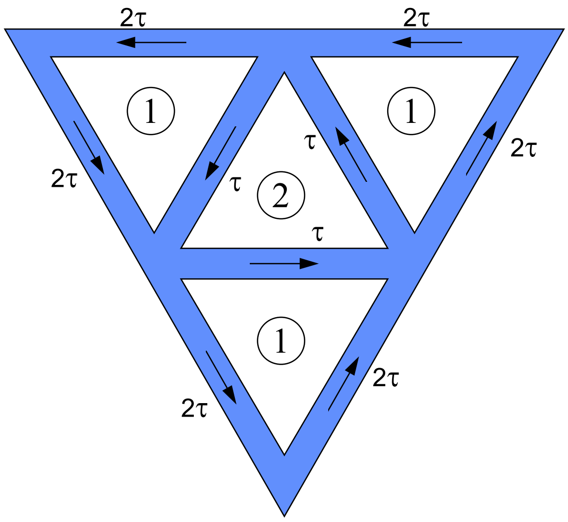

and express ϕ_1 and ϕ_2 in the torsion moment

$$\phi_1 = \tfrac{1}{3}\sqrt{3}\,\tfrac{4}{9}\frac{M_t}{a^2}$$

$$\phi_2 = \tfrac{1}{2}\sqrt{3}\,\tfrac{4}{9}\frac{M_t}{a^2}$$

In the outer walls of the girder, the shear stress is

$$\frac{\phi_1}{h} = \tfrac{4}{27}\sqrt{3}\,\frac{M_t}{a^2 h} = 2\tau$$

In the inner walls is the shear stress

$$\frac{\phi_2 - \phi_1}{h} = \frac{\tfrac{2}{9}\sqrt{3}\,\frac{M_t}{a^2} - \tfrac{4}{27}\sqrt{3}\,\frac{M_t}{a^2}}{h} = \tfrac{2}{27}\sqrt{3}\,\frac{M_t}{a^2 h} = \tau$$

d Warping

If warping is locally constrained, the girder will be stiffer than calculated above but not much because closed cross sections hardly warp.

Appendix 4. Calculation of a hollow-core slab

The hollow-core slab of this example was a Delft University exam problem (Elasticity theory 26 October 2001) [20]. The plate has 11 channels and is modelled as a thin wall closed cross section. Only 6 of the 12 webs have been included in the model. All walls have a thickness t.

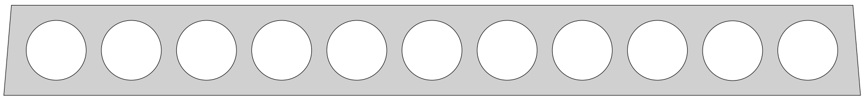

Cross section of a hollow-core slab

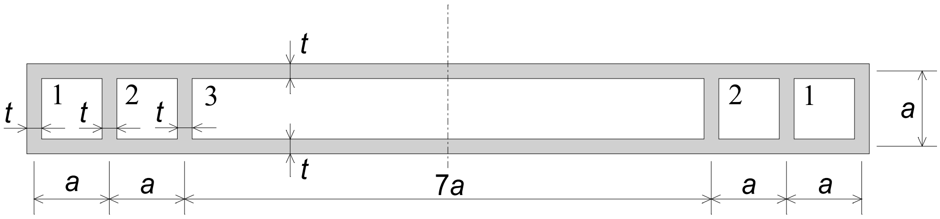

Model of the slab for calculation of the torsion properties

a The inner webs have been left out of the model. Why?

b Formulate the equilibrium equations of the membrane analogy. Use symmetry. (You do not need to simplify or solve the equations.)

c The equations have been solved with the following result.

$$w_1 = \frac{85}{232}\frac{pat}{S} \qquad w_2 = \frac{108}{232}\frac{pat}{S} \qquad w_3 = \frac{115}{232}\frac{pat}{S}$$

In this w_1 is the displacement of the weightless plate above cell 1, w_2 is that of cell 2 and w_3 is that of cell 3. In addition, S is the soap film stress and p is the pressure under the weightless plates.

Use this to calculate the torsion stiffness GI_t of the slab cross section.

d Calculate the shear stresses in the slab cross section as a function of the torsion moment and draw the shear stresses in the correct direction.

Answers

a Inner webs
The inner webs have been left out for two reasons. 1) They probably contribute little to the torsion properties. 2) Fewer equations need to be solved now.

b Equations

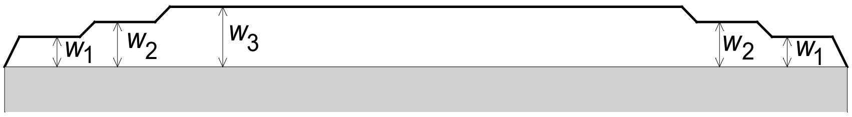

equilibrium of the plate above cell 1 $\quad pa^2 = 3a\,S\dfrac{w_1}{t} - a\,S\dfrac{w_2 - w_1}{t}$

cell 2 $\quad pa^2 = a\,S\dfrac{w_2 - w_1}{t} + 2a\,S\dfrac{w2}{t} - a\,S\dfrac{w_3 - w_2}{t}$

cell 3 $\quad pa\,7a = 2a\,S\dfrac{w_3 - w_2}{t} + 2(7a)S\dfrac{w_3}{t}$

c Torsion stiffness

From soap film to ϕ –hill with substitutions

$$w = \phi \qquad p = 2\theta \qquad S = \frac{1}{G}$$

Thus

$$\phi_1 = \frac{85}{232}2\theta Gat \qquad \phi_2 = \frac{108}{232}2\theta Gat \qquad \phi_3 = \frac{115}{232}2\theta Gat$$

The torsion moment is two times the content of the ϕ –hill.

$$M_t = 2\left(2\phi_1\,a^2 + 2\phi_2\,a^2 + \phi_3\,a(7a)\right)$$
$$M_t = 2\left(2\frac{85}{232}2\theta Gat\,a^2 + 2\frac{108}{232}2\theta Gat\,a^2 + \frac{115}{232}2\theta Gat\,a(7a)\right)$$
$$M_t = \frac{1191}{58}\theta Ga^3 t$$

For a wire frame model we use

$$M_t = GI_t\theta$$

Therefore, the torsion stiffness is

$$GI_t = \frac{1191}{58}Ga^3 t$$

d Shear stresses

The shear stress is the slope of the ϕ –hill. We rewrite the equation for the torsion moment

$$\theta Gat = \frac{M_t}{a^2}\frac{58}{1191}$$

and express ϕ_1, ϕ_2 and ϕ_3 in the torsion moment.

$$\phi_1 = \frac{85}{232}2\frac{M_t}{a^2}\frac{58}{1191} \qquad \phi_2 = \frac{108}{232}2\frac{M_t}{a^2}\frac{58}{1191} \qquad \phi_3 = \frac{115}{232}2\frac{M_t}{a^2}\frac{58}{1191}$$

$$\phi_1 = \frac{85}{2382}\frac{M_t}{a^2} \qquad \phi_2 = \frac{108}{2382}\frac{M_t}{a^2} \qquad \phi_3 = \frac{115}{2382}\frac{M_t}{a^2}$$

The shear stresses become

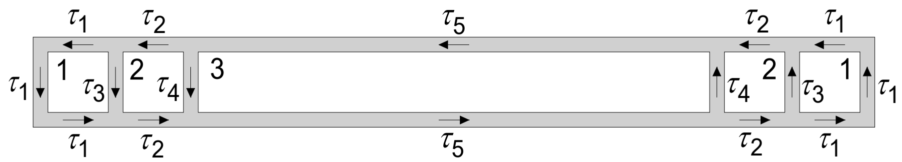

$$\tau_1 = \frac{\phi_1}{t} = \frac{85}{2382}\frac{M_t}{a^2 t}$$

$$\tau_2 = \frac{\phi_2}{t} = \frac{108}{2382}\frac{M_t}{a^2 t}$$

$$\tau_3 = \frac{\phi_2 - \phi_1}{t} = \frac{23}{2382}\frac{M_t}{a^2 t}$$

$$\tau_4 = \frac{\phi_3 - \phi_2}{t} = \frac{7}{2382}\frac{M_t}{a^2 t}$$

$$\tau_5 = \frac{\phi_3}{t} = \frac{115}{2382}\frac{M_t}{a^2 t}$$

<u>Encore</u> (not an exam question)
The graph below shows the torsion stiffness as a function of the number of webs n in the model. It appears that a model with just 4 webs is sufficiently accurate for calculation of the torsion stiffness.

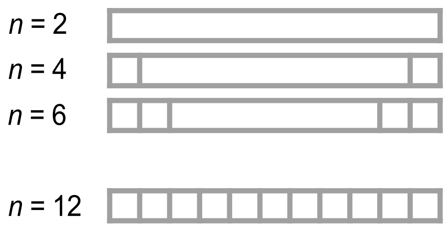

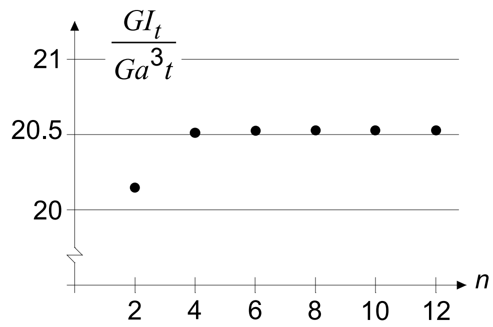

The largest shear stress converges less quickly with increasing n (not shown). But the model with 6 webs is sufficiently accurate. The largest shear stress in a model with 12 webs is $\tau_{max} = \frac{225}{4624}\frac{M_w}{a^2 t}$, which is just 0.8% larger than the model with 6 webs.

Appendix 5. Formulas for open thin wall cross sections [5]

The place of the shear centre is indicated with *O*.

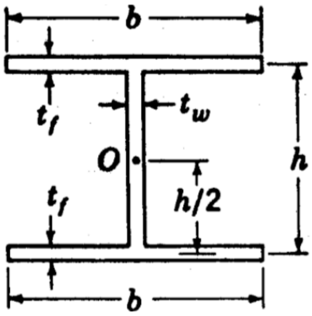

$$I_t = \frac{1}{3}(2bt_f^3 + ht_w^3)$$

$$C_w = \frac{1}{24} t_f b^3 h^2$$

$$\tau_{\max} = \frac{t M_t}{I_t} \qquad t = \max(t_f, t_w)$$

$$\sigma_{\max} = \frac{B}{\frac{1}{6} b^2 h t_f}$$

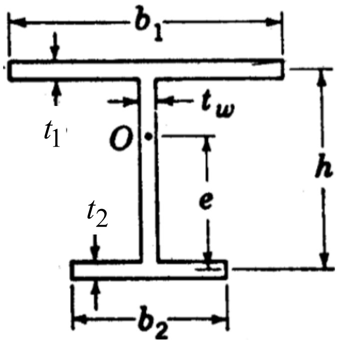

$$e = h \frac{b_1^3 t_1}{b_1^3 t_1 + b_2^3 t_2}$$

$$I_t = \frac{1}{3}\left(b_1 t_1^3 + b_2 t_2^3 + h t_w^3\right)$$

$$C_w = \frac{1}{12} h^2 \frac{b_1^3 t_1 b_2^3 t_2}{b_1^3 t_1 + b_2^3 t_2}$$

$$\sigma_{\max} = \frac{B}{\frac{1}{6} b_2^2 h t_2} \qquad \text{or} \qquad \sigma_{\max} = \frac{B}{\frac{1}{6} b_1^2 h t_1}$$

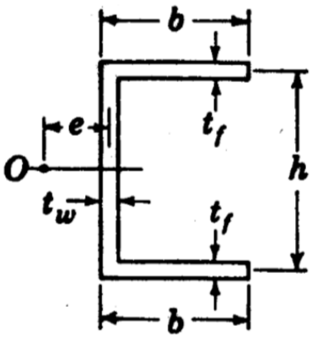

$$e = \frac{3b^2 t_f}{6bt_f + ht_w}$$

$$I_t = \frac{1}{3}(2bt_f^3 + ht_w^3)$$

$$C_w = \frac{1}{12} b^3 h^2 t_f \frac{3bt_f + 2ht_w}{6bt_f + ht_w}$$

$$\sigma_{\max} = \frac{B}{\frac{1}{6} b^2 h t_f \frac{3bt_f + 2ht_w}{3bt_f + ht_w}}$$

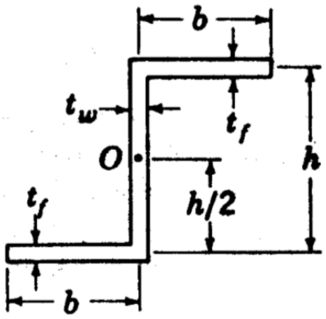

$$I_t = \frac{1}{3}(2bt_f^3 + ht_w^3)$$

$$C_w = \frac{1}{12} b^3 h^2 \frac{2t_f(b^2 + bh + h^2) + 3bht_w}{(2b+h)^2}$$

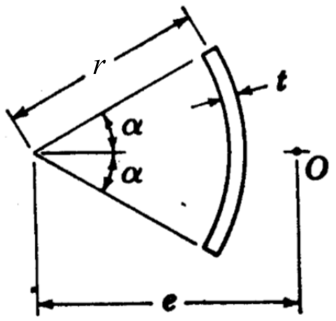

$$e = 2r\frac{\sin\alpha - \alpha\cos\alpha}{\alpha - \sin\alpha\cos\alpha}$$

$$I_t = \tfrac{2}{3} r\alpha t^3$$

$$C_w = \tfrac{2}{3} r^5 t(\alpha^3 - 6\frac{(\sin\alpha - \alpha\cos\alpha)^2}{\alpha - \sin\alpha\cos\alpha})$$

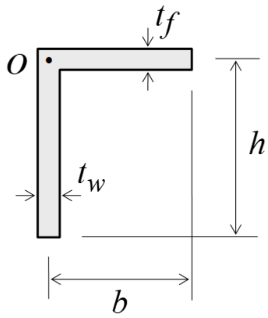

$$I_t = \tfrac{1}{3}(b t_f^3 + h t_w^3)$$

$$C_w = \tfrac{1}{36}(b^3 t_f^3 + h^3 t_w^3)$$

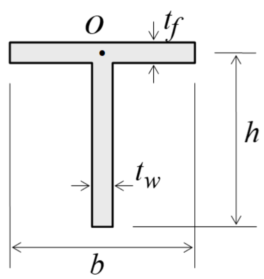

$$I_t = \tfrac{1}{3}(b t_f^3 + h t_w^3)$$

$$C_w = \tfrac{1}{36}(\tfrac{1}{4} b^3 t_f^3 + h^3 t_w^3)$$

More cross sections are in Roark's [2, table 21].

Appendix 6. Maple calculation of a box girder bridge with the Vlasov theory

```
> restart:
> l:=60:          # [m]
> ECw:=1183e9:    # [Nm4]
> GIt:=2690e8:    # [Nm2]
> mt:=0:          # [Nm/m]
> T:=269e5:       # [Nm]
>
> with(DEtools):
> ODE:=ECw*diff(phi(x),x,x,x,x)-GIt*diff(phi(x),x,x)=mt;
```

$$ODE := .1183\ 10^{13} \left(\frac{\partial^4}{\partial x^4} \phi(x) \right) - .2690\ 10^{12} \left(\frac{\partial^2}{\partial x^2} \phi(x) \right) = 0$$

```
> bound_con:= phi(0)=0, (D@@2)(phi)(0)=0, GIw*D(phi)(l/2)-
ECw*(D@@3)(phi)(l/2)=T/2, D(phi)(l/2)=0;
```

$$bound\_con := \phi(0) = 0, (\mathrm{D}^{(2)})(\phi)(0) = 0,$$
$$.2690\ 10^{12}\ \mathrm{D}(\phi)(30) - .1183\ 10^{13}\ (\mathrm{D}^{(3)})(\phi)(30) = .1345000000\ 10^{8}, \mathrm{D}(\phi)(30) = 0$$

```
> evalf(dsolve({ODE,bound_con},{phi(x)}));
```

$$\phi(x) = .00005000000000\ x + .6423299796\ 10^{-10}\ \mathbf{e}^{(-.4768521749\ x)} - .6423299796\ 10^{-10}\ \mathbf{e}^{(.4768521749\ x)}$$

```
> phi:=0.5000000000e-4*x-0.6423299796e-
10*exp(0.4768521749*x)+0.6423299796e-10*exp(-0.4768521749*x):
> B:=-ECw*diff(phi,x,x):
> Mt:=Re(GIt*diff(phi,x)+diff(B,x)):
> plot(phi(x),x=0..l/2);
```

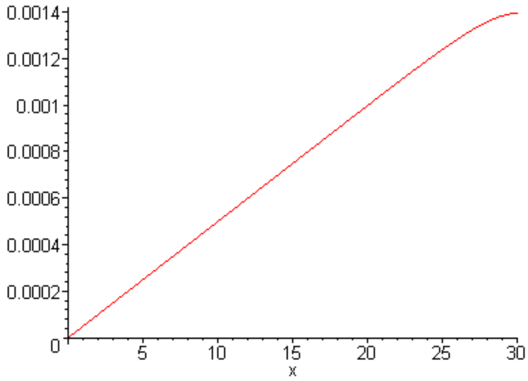


```
> plot(Mt,x=0..l/2);
```

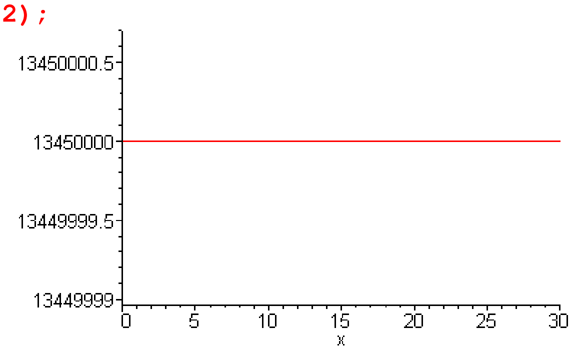


```
> plot(B,x=0..l/2);
```

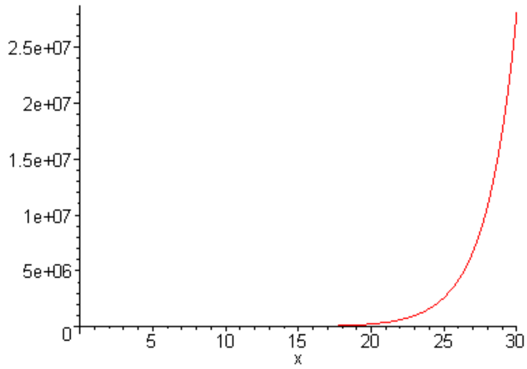


```
> x:=1/2: simplify(B); simplify(phi);
```

$$.2820580643\ 10^{8}$$

$$.001395145701$$

Appendix 7. Maple calculation of a cantilever with the Vlasov theory

```
> restart:
> l:=2540:              # [mm]
> ECw:=207000*191e8:    # [Nmm4]
> GIt:=79300*278000:    # [Nmm2]
> mt:=0:                # [Nmm/mm]
> T:=2.26e6:            # [Nmm]
>
> with(DEtools):
> ODE:=ECw*diff(phi(x),x,x,x,x)-GIw*diff(phi(x),x,x)=mt;
```

$$ODE := 0.39537000 10^{16} \left(\frac{d^4}{dx^4} \phi(x) \right) - 22045400000 \left(\frac{d^2}{dx^2} \phi(x) \right) = 0$$

```
> bound_con:= phi(0)=0, D(phi)(0)=0, GIw*D(phi)(l)-
ECw*(D@@3)(phi)(l)=T, (D@@2)(phi)(l)=0;
```

$$bound\_con := \phi(0) = 0, \mathrm{D}(\phi)(0) = 0,$$
$$22045400000 \mathrm{D}(\phi)(2540) - 0.39537000 10^{16} (\mathrm{D}^{(3)})(\phi)(2540) = 0.226 \, 10^7,$$
$$(\mathrm{D}^{(2)})(\phi)(2540) = 0$$

```
> evalf(dsolve({ODE,bound_con},{phi(x)}));
```

$$\phi(x) = -0.04341381587 + 0.0001025157176 x - 0.2679299633 10^{-6} \, \mathbf{e}^{(0.002361332449 \; x)}$$
$$+ 0.04341408381 \mathbf{e}^{(-0.002361332449 \; x)}$$

```
> phi:=-.4154442895e-1+.9810141906e-4*x-.2563929731e-
6*exp(.2361332449e-2*x)+.4154468535e-1*exp(-.2361332449e-2*x):
> B:=-ECw*diff(phi,x,x):
> Mt1:=GIt*diff(phi,x):
> Mt2:=diff(B,x):
> plot(phi,x=0..l);
```

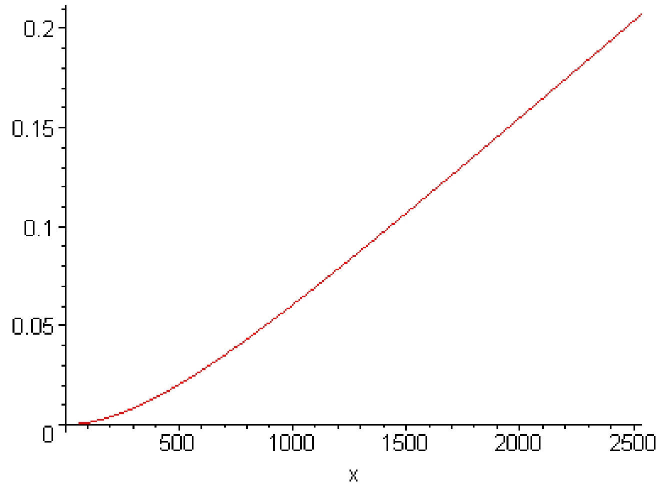


```
> plot(B,x=0..l);
```

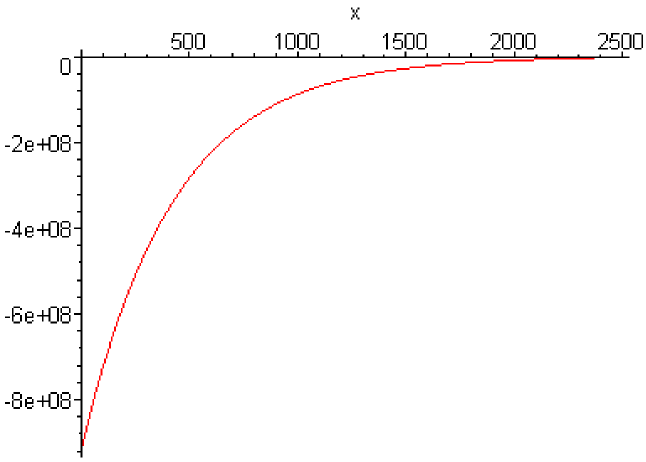


```
> plot({Mt2,Mt1+Mt2},x=0..l);
```

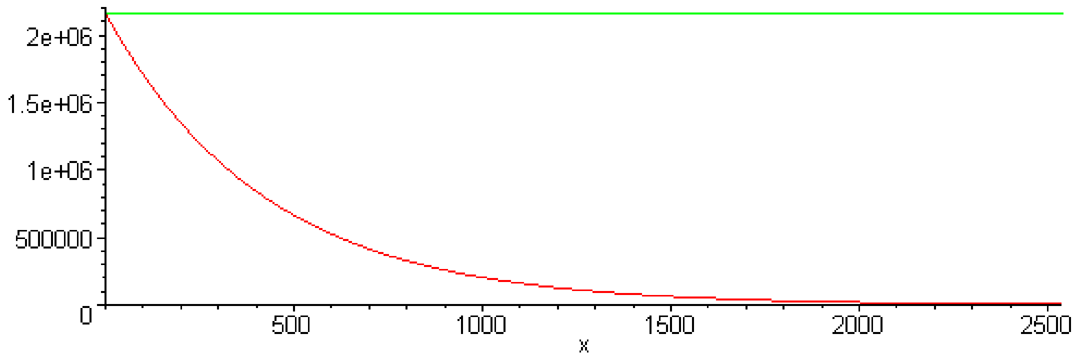

Appendix 8. Calculation of torsion stresses in an I section

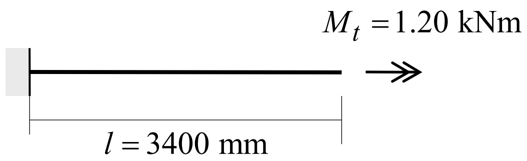

Figure. Cantilever loaded in torsion

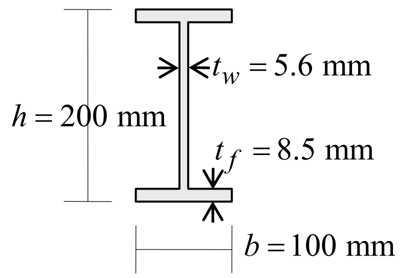

Cross-section, IPE 200

Young's modulus $E = 2.1\ 10^5$ N/mm²
Poisson's ratio $\nu = 0.35$

Shear modulus $G = \dfrac{E}{2(1+\nu)} = 77777$ N/mm²

Torsion constant $I_t = \frac{1}{3}(h - t_f)t_w^3 + \frac{2}{3}bt_f^3 = 52152$ mm^4

Warping constant $C_w = \frac{1}{24}t_f\,(h - t_f)^2 b^3 = 1299\ 10^7$ mm^6

Characteristic length $l_c = \sqrt{\dfrac{E\,C_w}{G\,I_t}} = 820.0$ mm

In general, a torsion moment causes shear stresses and it can cause normal stresses. In cross-sections that can warp freely only shear stresses occur. This happens in the free end of the cantilever. The largest shear stress is

$$\tau_{\max} = \frac{M_t\,t_f}{I_t} = 196 \text{ N/mm}^2.$$

The Von Mises stress is $\sqrt{3\,\tau_{\max}^2}$ = 339 N/mm².

In cross-sections that cannot warp mostly normal stresses occur. This happens at the fixed end of the cantilever. The bi-moment is

$$B = l_c M_t = 9840\ 10^5 \text{ Nmm}^2,$$

which is accurate if $l_c < \frac{1}{3}l$, which is fulfilled. The largest normal stress in this section is

$$\sigma_{\max} = \frac{B}{\frac{1}{6}(h - t_f)\,t_f\,b^2} = 363 \text{ N/mm}^2.$$

This stress occurs at the left and right of the flanges both in compression and tension.

The rotation at the free end is

$$\varphi = \frac{M_t}{GI_t}\left(l - l_c \tanh\frac{l}{l_c}\right) = 0.763 \text{ rad}.$$

It needs to be mentioned that from a plastic point of view the stresses due to the bi-moment can be neglected because just the shear stresses are an equilibrium system that can carry the load.

Check

A finite element analysis was made with ANSYS 11. Applied are 20 node brick shaped elements (solid95). At the fixed end all degrees of freedom have zero displacement imposed. At the free end the torsion loading is applied by 6 forces. The model consists of 959820 degrees of freedom. A linear elastic analysis was performed (31 minutes on a Pentium 4 PC).

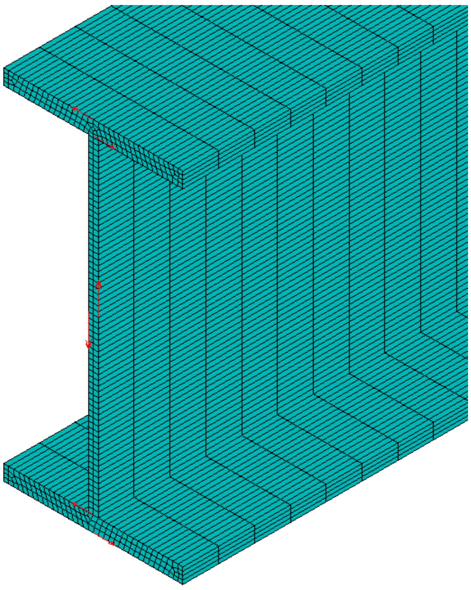

Figure. Mesh and torsion loading (red arrows) at the free end of the cantilever

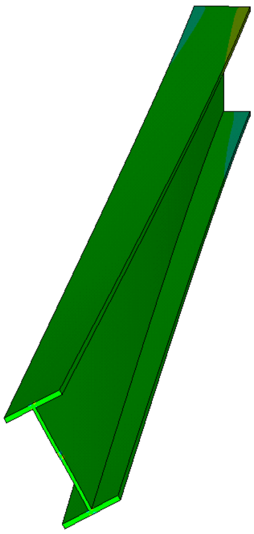

Figure. Torsion deformation

The horizontal displacement of nodes in the free ends of the flanges are –87.3 mm and 87.3 mm. Therefore, the rotation is

$$\varphi = \frac{87.3 + 87.3}{200} = 0.873 \text{ rad}.$$

The hand calculation result is 13% smaller. This might be caused by shear deformation of the flanges.

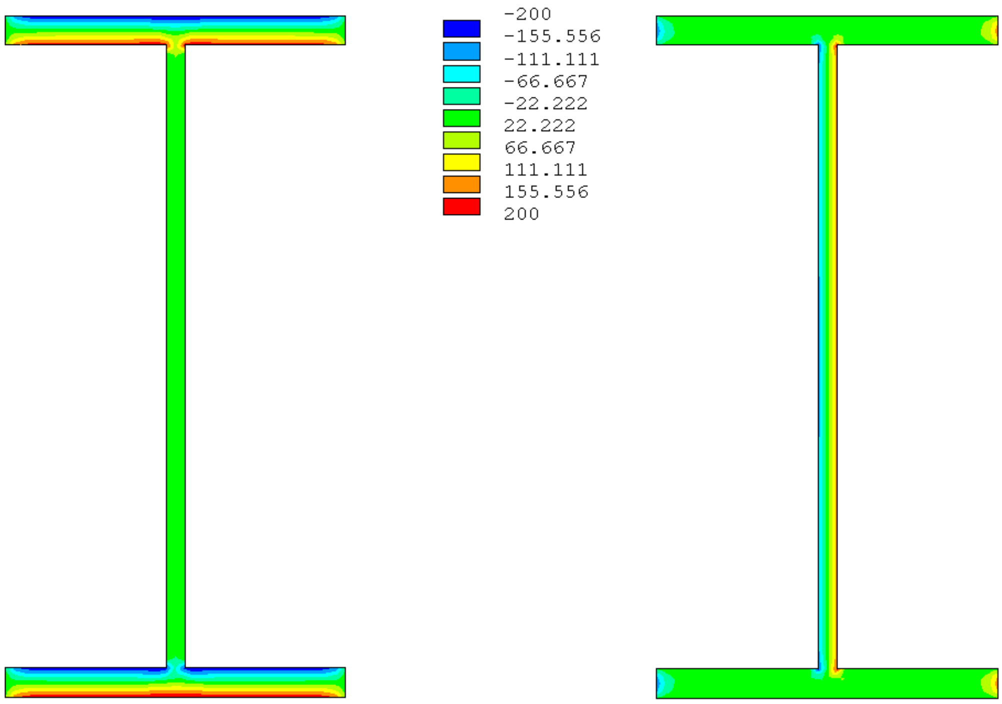

Figure. Horizontal and vertical shear stresses in a cross-section 300 mm from the free end

The stresses in the re-entrant corners of the cross-section are ignored. (In theory the sharp corners have infinitely large stresses.) The largest shear stress in the free end cross-section is 200 N/mm². The hand calculation result is 2% smaller.

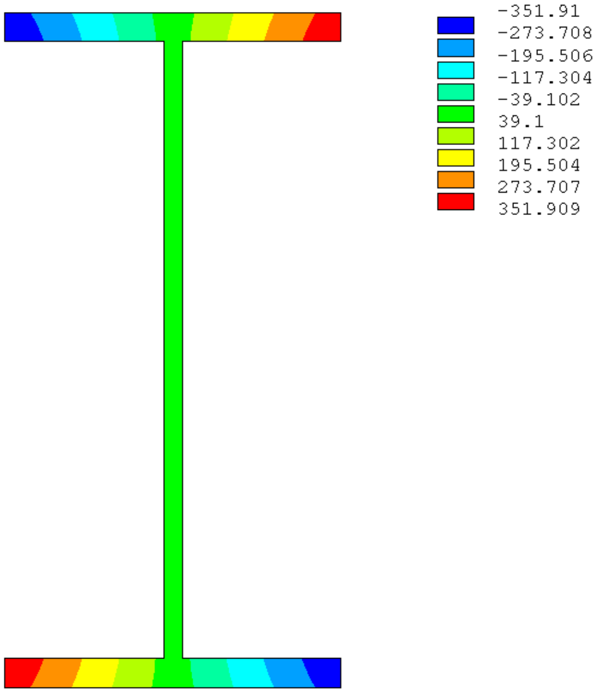

Figure. Normal stresses in a cross-section 50 mm from the fixed end

The largest normal stress in the fixed end cross-section is 352 N/mm². The hand calculation result is 3% larger. The differences between the results of the hand calculation and the finite element analysis are acceptable for most purposes.

Appendix 9. Stiffness matrix of a frame element

In some frame programs the torsion properties have not been implemented correctly. To help software developers, this appendix gives the stiffness matrix consistent with the torsion theory of Saint-Venant. The *x* axis is in the direction of the beam or column. The *y* and *z* axis are the principal directions of the cross section. e_y and e_z are the coordinates of the shear centre. I_{yy} is the moment of inertia of the cross section in the *y* direction and I_{zz} is the moment of inertia in the *z* direction. Shear deformation has been neglected.

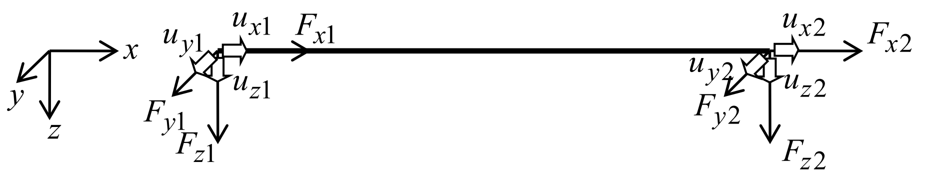

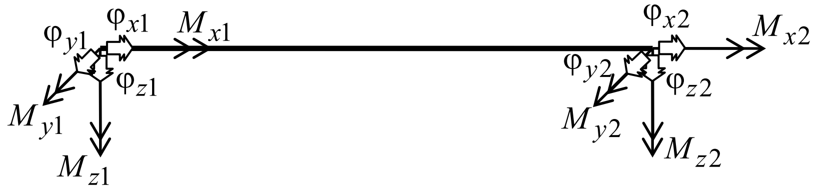

$$
\begin{bmatrix} F_{x1} \\ F_{y1} \\ F_{z1} \\ M_{x1} \\ M_{y1} \\ M_{z1} \\ F_{x2} \\ F_{y2} \\ F_{z2} \\ M_{x2} \\ M_{y2} \\ M_{z2} \end{bmatrix}
=
\begin{bmatrix}
\frac{EA}{l} & 0 & 0 & 0 & 0 & 0 & -\frac{EA}{l} & 0 & 0 & 0 & 0 & 0 \\
. & 12\frac{EI_{yy}}{l^3} & 0 & -e_z 12\frac{EI_{yy}}{l^3} & 0 & 6\frac{EI_{yy}}{l^2} & 0 & -12\frac{EI_{yy}}{l^3} & 0 & e_z 12\frac{EI_{yy}}{l^3} & 0 & 6\frac{EI_{yy}}{l^2} \\
. & . & 12\frac{EI_{zz}}{l^3} & e_y 12\frac{EI_{zz}}{l^3} & -6\frac{EI_{zz}}{l^2} & 0 & 0 & 0 & -12\frac{EI_{zz}}{l^3} & -e_y 12\frac{EI_{zz}}{l^3} & -6\frac{EI_{zz}}{l^2} & 0 \\
. & . & . & \frac{GI_t}{l} + e_z^2 12\frac{EI_{yy}}{l^3} + e_y^2 12\frac{EI_{zz}}{l^3} & -e_y 6\frac{EI_{zz}}{l^2} & -e_z 6\frac{EI_{yy}}{l^2} & 0 & e_z 12\frac{EI_{yy}}{l^3} & -e_y 12\frac{EI_{zz}}{l^3} & -\frac{GI_t}{l} - e_z^2 12\frac{EI_{yy}}{l^3} - e_y^2 12\frac{EI_{zz}}{l^3} & -e_y 6\frac{EI_{zz}}{l^2} & -e_z 6\frac{EI_{yy}}{l^2} \\
. & . & . & . & 4\frac{EI_{zz}}{l} & 0 & 0 & 0 & 6\frac{EI_{zz}}{l^2} & e_y 6\frac{EI_{zz}}{l^2} & 2\frac{EI_{zz}}{l} & 0 \\
. & . & . & . & . & 4\frac{EI_{yy}}{l} & 0 & -6\frac{EI_{yy}}{l^2} & 0 & e_z 6\frac{EI_{yy}}{l^2} & 0 & 2\frac{EI_{yy}}{l} \\
. & . & . & . & . & . & \frac{EA}{l} & 0 & 0 & 0 & 0 & 0 \\
. & . & . & \text{sym.} & . & . & . & 12\frac{EI_{yy}}{l^3} & 0 & -e_z 12\frac{EI_{yy}}{l^3} & 0 & -6\frac{EI_{yy}}{l^2} \\
. & . & . & . & . & . & . & . & 12\frac{EI_{zz}}{l^3} & e_y 12\frac{EI_{zz}}{l^3} & 6\frac{EI_{zz}}{l^2} & 0 \\
. & . & . & . & . & . & . & . & . & \frac{GI_t}{l} + e_z^2 12\frac{EI_{yy}}{l^3} + e_y^2 12\frac{EI_{zz}}{l^3} & e_y 6\frac{EI_{zz}}{l^2} & e_z 6\frac{EI_{yy}}{l^2} \\
. & . & . & . & . & . & . & . & . & . & 4\frac{EI_{zz}}{l} & 0 \\
. & . & . & . & . & . & . & . & . & . & . & 4\frac{EI_{yy}}{l}
\end{bmatrix}
\begin{bmatrix} u_{x1} \\ u_{y1} \\ u_{z1} \\ \varphi_{x1} \\ \varphi_{y1} \\ \varphi_{z1} \\ u_{x2} \\ u_{y2} \\ u_{z2} \\ \varphi_{x2} \\ \varphi_{y2} \\ \varphi_{z2} \end{bmatrix}
$$

The matrix can checked in the following way. A rotation η around the shear centre at node 2 gives $\varphi_{x2} = \eta$, $u_{y2} = e_z \eta$, $u_{z2} = -e_y \eta$. The other displacements and rotations are zero. Substitution in the matrix gives $M_{x1} = -\frac{GI_w}{l}\eta$, $M_{x2} = \frac{GI_w}{l}\eta$. The other forces and moments are zero. This is the correct result.

The latter stiffness matrix can be extended with shear deformation and constrained warping. In addition, the y and z axes do not need to point in the principal directions and the element can be translated over distances s_y and s_z compared to the nodes. Moreover, linearly distributed loads q_x, q_y and q_z can be applied and a linearly distributed torsion moment m_x can be applied. The result is not shown here because it does not fit on one page. The Maple script below produces the 14×14 elements of the stiffness matrix. These can be copied to Fortran or another language in which a frame program is writen.

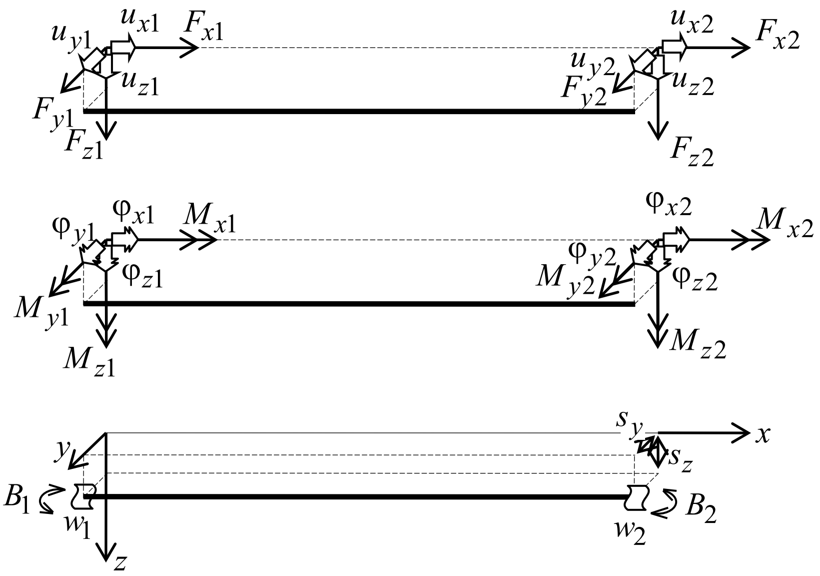

$$
\begin{bmatrix} F_{x1} \\ F_{y1} \\ F_{z1} \\ M_{x1} \\ M_{y1} \\ M_{z1} \\ B_1 \\ F_{x2} \\ F_{y2} \\ F_{z2} \\ M_{x2} \\ M_{y2} \\ M_{z2} \\ B_2 \end{bmatrix}
=
\begin{bmatrix} N_1 \\ N_2 \\ N_3 \\ N_4 \\ N_5 \\ N_6 \\ N_7 \\ N_8 \\ N_9 \\ N_{10} \\ N_{11} \\ N_{12} \\ N_{13} \\ N_{14} \end{bmatrix}
+
\begin{bmatrix} K_{1,1} & K_{1,2} & & & K_{1,14} \\ & K_{2,2} & & & \\ & & K_{3,3} & & \\ & & & & \\ & & sym. & & \\ & & & & K_{14,14} \end{bmatrix}
\begin{bmatrix} u_{x1} \\ u_{y1} \\ u_{z1} \\ \varphi_{x1} \\ \varphi_{y1} \\ \varphi_{z1} \\ w_1 \\ u_{x2} \\ u_{y2} \\ u_{z2} \\ \varphi_{x2} \\ \varphi_{y2} \\ \varphi_{z2} \\ w_2 \end{bmatrix}
$$

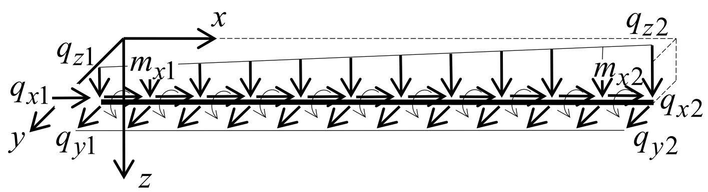

Note that there is a restriction to connecting elements. The warping can only be connected when elements have the same cross section and are in line with each other. If not, one must choose for no warping ($w = 0$) or no bi moment ($B = 0$).

```
> restart: # Frame element stiffness matrix including constrained warping
> # The element has 3 lines: 1) structure line, 2) normal force centre line, 3) shear
> force centre line. The normal force centre line is offset by sy, sz to the structure
> centre line. The shear centre line is offset by ey, ez to the normal force centre
line
> qx:=qx1*(1-x/l)+qx2*x/l:        # load on the normal force centre line
> qy:=qy1*(1-x/l)+qy2*x/l:
> qz:=qz1*(1-x/l)+qz2*x/l:
> mx:=mx1*(1-x/l)+mx2*x/l:
> e:=diff(ux(x),x):               # axial strain of the structure centre line
> phiy:=gy(x)-diff(uy(x),x):      # rotations of a section. g is the shear deformation
> phiz:=gz(x)-diff(uz(x),x):
> Ky:=diff(phiy,x):               # curvatures
> Kz:=diff(phiz,x):
> N:=EA*e+EA*sy*Ky+EA*sz*Kz:      # normal force and moments
> My:=EA*sy*e+EIyy*Ky+EIyz*Kz:
> Mz:=EA*sz*e+EIyz*Ky+EIzz*Kz:
> Vy:=GAy*gy(x):                  # shear forces
> Vz:=GAz*gz(x):
> B:=-ECw*diff(phi(x),x,x):       # bi moment
>                                 # phi is the rotation around the shear centre line
> Mx:=GIw*diff(phi(x),x)+diff(B,x)+Vz*ey-Vy*ez: # torsion moment
> DE1:= diff(N,x)+qx=0:
> DE2:= diff(Vy,x)+qy=0:
> DE3:= diff(Vz,x)+qz=0:
> DE4:= diff(Mx,x)+mx=0:
> DE5:= diff(My,x)-Vy=0:
> DE6:= diff(Mz,x)-Vz=0:
> BC1:= ux1=ux(0), ux2=ux(l):
> BC2:= uy1=uy(0)+phi(0)*(sz+ez), uy2=uy(l)+phi(l)*(sz+ez), phiz1=-gy(0)+D(uy)(0),
phiz2=-gy(l)+D(uy)(l):
> BC3:= uz1=uz(0)-phi(0)*(sy+ey), uz2=uz(l)-phi(l)*(sy+ey), phiy1= gz(0)-D(uz)(0),
phiy2= gz(l)-D(uz)(l):
> BC4:= phix1=phi(0), phix2=phi(l), w1=D(phi)(0), w2=D(phi)(l):
> Opl:=dsolve({DE1,DE2,DE3,DE4,DE5,DE6,
BC1,BC2,BC3,BC4},{ux(x),uy(x),uz(x),phi(x),gy(x),gz(x)}): assign(Opl):
> e:=diff(ux(x),x):
> phiy:=gy(x)-diff(uy(x),x):
> phiz:=gz(x)-diff(uz(x),x):
> Ky:=diff(phiy,x):
> Kz:=diff(phiz,x):
> N:=EA*e+EA*sy*Ky+EA*sz*Kz:
> My:=EA*sy*e+EIyy*Ky+EIyz*Kz:
> Mz:=EA*sz*e+EIyz*Ky+EIzz*Kz:
> Vy:=GAy*gy(x):
> Vz:=GAz*gz(x):
> B:=-ECw*diff(phi(x),x,x):
> Mx:=GIw*diff(phi(x),x)+diff(B,x)+Vz*ey-Vy*ez:
> x:=0: Fx1:=-N: Fy1:=-Vy: Fz1:=-Vz: Mx1:=-Mx: My1:=-Mz: Mz1:=My:  B1:=B:  x:='x':
> x:=l: Fx2:=N:  Fy2:=Vy:  Fz2:=Vz:  Mx2:= Mx: My2:=Mz:  Mz2:=-My: B2:=-B: x:='x':
> K[1,1]:=simplify(diff(Fx1,ux1)):
> K[1,2]:=simplify(diff(Fx1,uy1)):
> K[2,2]:=simplify(diff(Fy1,uy1)):
> K[14,14]:=simplify(diff(B2,w2)):
> # etc.
> ux1:=0: uy1:=0: uz1:=0: phix1:=0: phiy1:=0: phiz1:=0: w1:=0:
> ux2:=0: uy2:=0: uz2:=0: phix2:=0: phiy2:=0: phiz2:=0: w2:=0:
> N[1]:=simplify(Fx1):
> N[2]:=simplify(Fy1):
> # etc.
>
>
```

Appendix 10. Derivation of Vlasov's theory

In this appendix the equations of the torsion theory of Vlasov are derived.

Ingredients

The following definitions are used.

strain	$\varepsilon_{xx} = \dfrac{\partial u_x}{\partial x}$	[4]	(1)
warping	$u_x = \Psi\,\theta$	(p. 5)	(2)
torsion deformation	$\theta = \dfrac{d\varphi}{dx}$	(p. 5)	(3)
shear stresses	$\tau_{xy} = \tau_{xyS} + \tau_{xyV}$ $\tau_{xz} = \tau_{xzS} + \tau_{xzV}$		(4)
	$\tau_{xyS} = G(\dfrac{\partial\Psi}{\partial y} - z)\theta$ $\tau_{xzS} = G(\dfrac{\partial\Psi}{\partial z} + y)\theta$	(p. 6)	(5)
boundary condition	$\tau_{xy}\dfrac{dz}{dS} - \tau_{xz}\dfrac{dy}{dS} = 0$	[4]	(6)
torsion moment	$M_{tS} = \int_A (y\,\tau_{xzS} - z\,\tau_{xyS})dA$	(p. 6)	(7)
	$M_{tV} = \int_A (y\,\tau_{xzV} - z\,\tau_{xyV})dA$		(8)
	$M_t = M_{tS} + M_{tV}$		(9)
	$m_t + \dfrac{dM_t}{dx} = 0$		(10)
	$M_{tS} = GI_t\theta$	(p. 3)	(11)
bi moment	$B = -\int_A \sigma_{xx}\Psi\, dA$	(p. 24)	(12)
warping constant	$C_w = \int_A \Psi^2 dA$	(p. 24)	(13)

One of the equilibrium equations of linear elastic material is

$$\frac{\partial\sigma_{xx}}{\partial x} + \frac{\partial\tau_{xy}}{\partial y} + \frac{\partial\tau_{xz}}{\partial z} = 0 \qquad [4] \qquad (14)$$

One of the constitutive equations of linear elastic materials is

$$\varepsilon_{xx} = \frac{\sigma_{xx}}{E} - \nu\frac{\sigma_{yy}}{E} - \nu\frac{\sigma_{zz}}{E}. \qquad [4]$$

In beams the stresses perpendicular to the surface are small and neglegible. So $\sigma_{yy} = \sigma_{zz} = 0$. Substitution in the previous equation gives

$$\sigma_{xx} = E\,\varepsilon_{xx} . \tag{15}$$

Approximation

It is assumed that $\frac{1}{G\theta}\int_A (\tau_{xyS}\tau_{xyV} + \tau_{xzS}\tau_{xzV})dA$ is much smaller than the torsion moment in a beam cross section.

$$\frac{1}{G\theta}\int_A (\tau_{xyS}\tau_{xyV} + \tau_{xzS}\tau_{xzV})dA \ll M_t \tag{16}$$

This is fulfilled for thin wall open cross sections. This follows from figure 40: the Saint-Venant stress flows partially with the Vlasov stress and partially against the Vlasov stress. The with and against contribution to the integral cancel each other out.

For other cross-sections the accuracy of this approximation is not clear. Note that the Vlasov theory shows that constrained warping for closed and solid cross sections is often neglegeble. However, the unclearness above makes the conclusion less hard. More research is needed.

Derivation

Substitution of equation 1, 2 and 3 in 15 gives

$$\sigma_{xx} = E\Psi \frac{d^2\varphi}{dx^2} . \tag{17}$$

Substitution of this in equation 12 using equation 13 gives

$$\boxed{B = -EC_w \frac{d^2\varphi}{dx^2}} \tag{18}$$

Substitution of this in equation 17 gives

$$\boxed{\sigma_{xx} = -\frac{B\Psi}{C_w}} \tag{19}$$

Substitution of this in equation 14 gives

$$\frac{\partial\tau_{xyV}}{\partial y} + \frac{\partial\tau_{xzV}}{\partial z} = \frac{\partial B}{\partial x}\frac{\Psi}{C_w} .$$

$$\int_A \left(\frac{\partial \tau_{xyV}}{\partial y} + \frac{\partial \tau_{xzV}}{\partial z}\right)\Psi \, dA = \int_A \frac{dB}{dx}\frac{\Psi^2}{C_w} dA \, .$$

Application of the product rule $\frac{\partial \tau_{xyV}\Psi}{\partial y} = \tau_{xyV}\frac{\partial \Psi}{\partial y} + \frac{\partial \tau_{xyV}}{\partial y}\Psi$ and equation 13 gives

$$\int_A \left(\frac{\partial \tau_{xyV}\Psi}{\partial y} - \tau_{xyV}\frac{\partial \Psi}{\partial y} + \frac{\partial \tau_{xzV}\Psi}{\partial z} - \tau_{xzV}\frac{\partial \Psi}{\partial z}\right) dA = \frac{dB}{dx} \, .$$

Green theorem is $\int_A \left(\frac{\partial \tau_{xyV}\Psi}{\partial y} + \frac{\partial \tau_{xzV}\Psi}{\partial z}\right) dA = \oint_S \left(\tau_{xyV}\Psi\frac{dz}{dS} - \tau_{xzV}\Psi\frac{dy}{dS}\right) dS$
which is equal to zero because of equation 6. (The Saint-Venant stresses already comply with the boundary condition therefore the Vlasov stresses must also comply.) Application of this gives

$$-\int_A \left(\tau_{xyV}\frac{\partial \Psi}{\partial y} + \tau_{xzV}\frac{\partial \Psi}{\partial z}\right) dA = \frac{dB}{dx} \, .$$

Substitution of equation 5 gives

$$-\int_A \left(\tau_{xyV}\left(\frac{\tau_{xyS}}{G\theta} + z\right) + \tau_{xzV}\left(\frac{\tau_{xzS}}{G\theta} - y\right)\right) dA = \frac{dB}{dx} \, .$$

This can be written as

$$\int_A (y\,\tau_{xzV} - z\,\tau_{xyV}) dA = \frac{1}{G\theta}\int_A (\tau_{xyV}\tau_{xyS} + \tau_{xzV}\tau_{xzS}) dA + \frac{dB}{dx} \, .$$

Application of equation 8 and 17 gives

$$M_{tV} = \frac{dB}{dx} \, .$$

Substitution of this and equation 11 in equation 9 gives

$$\boxed{M_t = GI_t\frac{d\varphi}{dx} + \frac{dB}{dx}} \qquad (20)$$

Substitution of equation 18 in 20 and the result in equation 10 gives

$$\boxed{EC_w\frac{d^4\varphi}{dx^4} - GI_t\frac{d^2\varphi}{dx^2} = m_t} \qquad (21)$$

Q.E.D.